

5-2013

Characterization of Potential Wear Sources in Knee Arthroplasty Prostheses After In Vivo Function

Nicole Durig

Clemson University, ndurig334@gmail.com

Follow this and additional works at: https://tigerprints.clemson.edu/all_theses

 Part of the [Biomedical Engineering and Bioengineering Commons](#)

Recommended Citation

Durig, Nicole, "Characterization of Potential Wear Sources in Knee Arthroplasty Prostheses After In Vivo Function" (2013). *All Theses*. 1617.

https://tigerprints.clemson.edu/all_theses/1617

This Thesis is brought to you for free and open access by the Theses at TigerPrints. It has been accepted for inclusion in All Theses by an authorized administrator of TigerPrints. For more information, please contact kokeefe@clemson.edu.

CHARACTERIZATION OF POTENTIAL WEAR SOURCES IN KNEE
ARTHROPLASTY PROSTHESES AFTER IN VIVO FUNCTION

A Thesis
Presented to
the Graduate School of
Clemson University

In Partial Fulfillment
of the Requirements for the Degree
Master of Science
Bioengineering

by
Nicole Elizabeth Durig
May 2013

Accepted by:
Melinda Harman, Ph.D., Committee Chair
Brandon Broome, M.D.
Randy Hutchison, Ph.D.
Amir Poursaee, Ph.D.

ABSTRACT

Total joint arthroplasty (TJA) is a common procedure generally performed in patients with osteoarthritis. While TJA continues to be a successful treatment for degenerative joint disease, there are many studies that demonstrate wear and its sequelae as the major limitation of joint replacement longevity. Previous studies have shown that wear debris originates from four main locations: articulating surfaces, modular component surfaces, surfaces of fixation, and adjuvant fixation devices. [14, 57, 70] Each of these possible wear sources can initiate the cascade of failure associated with wear-induced osteolysis and lead to subsequent revision surgery. The objective of this thesis is to characterize the *in vivo* performance of knee prostheses by quantitatively assessing performance at different potential wear-inducing interactions, including bearing surfaces and modular articular surfaces. The objective will be accomplished through three studies that will aim to investigate different wear modes.

The purpose of Study 1 is to explore the relationships between femoral component surface roughness, polyethylene insert damage and *in vivo* duration through the evaluation of metal-polymer UKA bearing couples that were retrieved after 1 to 19 years of *in vivo* service. This study characterizes the distribution of damage on matched metal-polymer bearing couples of retrieved UKA and quantifies ranges of surface roughness corresponding to the different damage modes visually identified on both bearing surfaces. The purpose of Study 2 is to characterize the damage of retrieved knee replacement bearing couples that have experienced complete polyethylene wear-through, while considering the material properties of common alloys used to fabricate femoral

components and tibial baseplates, including cobalt-chrome alloy, titanium alloy, and oxidized zirconium alloy. The purpose of Study 3 is to evaluate the clinical outcomes of 84 patients implanted with primary TKA prostheses of a single design that utilizes a Morse taper feature for attaching a modular tibial stem. The results from this thesis provide clinically relevant data for understanding the performance of knee prosthesis designs under physiologic conditions. Additionally, this thesis provides relevant surface roughness values for prostheses with in vivo function for assessing the predictive capabilities of in vitro simulation and analytical models.

DEDICATION

I dedicate this work, primarily, to my four sisters, Mallory, Delaney and Meagan Durig and Hope Marie Mitchell, who inspire and amaze me daily. Also, to my parents, family, and friends for all of their love, support and encouragement.

ACKNOWLEDGMENTS

I would like to thank my advisor, Dr. Melinda Harman, for her guidance, support and patience throughout my research experience. It has been an invaluable experience as a student to work with such a well-established, knowledgeable researcher in the field of orthopaedics. I also would like to thank my committee, Dr. Brandon Broome, Dr. Randy Hutchison, and Dr. Amir Poursaee, for their guidance and support throughout my research. To Dr. Thomas Pace, Dr. John DesJardins, Dr. Estefania Alvarez and Chad Valitchka, I thank you for all of your assistance and support. Dr. Sabine Schmitt and Dr. Andrew Hodge also have been invaluable to my research for supplying the prostheses to make these projects possible. Finally, I would like to thank the members, faculty, and staff of RE-MED laboratory, CU-REPRO, CUBEInc., and the Department of Bioengineering, without whose help and support I would not have been able to accomplish all that I have.

TABLE OF CONTENTS

	Page
TITLE PAGE	i
ABSTRACT	ii
DEDICATION	iv
ACKNOWLEDGMENTS	v
LIST OF TABLES	viii
LIST OF FIGURES	iv
CHAPTER	
I. INTRODUCTION	1
Knee Arthroplasty	1
Unicondylar versus Total Knee Arthroplasty	5
Wear of Arthroplasty Prostheses	9
Purpose.....	15
II. Study 1: Mode I Wear.....	17
Introduction.....	17
Materials and Methods.....	28
Results.....	37
Discussion.....	42
III. Study 2: Mode II Wear	48
Introduction.....	48
Materials and Methods.....	52
Results.....	61
Discussion.....	68
IV. Study 3: Mode IV Wear Model	73
Introduction.....	73
Materials and Methods.....	78

Table of Contents (Continued)

	Page
Results.....	83
Discussion.....	85
V. ENGINEERING SIGNIFICANCE.....	87
Study 1: Mode I Wear.....	87
Study 2: Mode II Wear	90
Study 3: Mode IV Wear Model	94
VI. CONCLUSIONS & FUTURE STUDIES	97
REFERENCES	101

LIST OF TABLES

Table		Page
2.1	Available data on retrieved UKA	29
2.2	Available clinical data for patient population.....	31
2.3	Description of collected surface roughness parameters.....	36
2.4	UKA femoral component visual damage modes, zone coverage and corresponding roughness values, displayed as mean \pm standard deviation (range).....	42
2.5	Reported surface roughness values and current study median values with associated range	44
3.1	Material properties of typical materials used to fabricate components of TKA and UKA	49
3.2	Available data on retrieved UKA and TKA prostheses.....	54
3.3	Material composition of UKA and TKA prostheses components	56
3.4	Available clinical data for patient population.....	57
3.5	Roughness values for varying potential metal-on-metal bearing couples of TKA and UKA	63
3.6	Femoral component visual damage modes, zone coverage and corresponding roughness values, displayed as mean \pm standard deviation (range) of each of the 8 condyles of TKA and 3 UKA characterized	68
5.1	The top part of the table demonstrates the equations to determine contact area and contact pressure of both the line and point contacts. The bottom part of the table shows the equations to find the surface stress of the different contacts within the contact region	91

LIST OF FIGURES

Figure	Page
1.1 Typical total knee arthroplasty component.....	2
1.2 Image demonstrating differences between TKA and UKA.....	3
1.3 Projected number of total knee arthroplasties performed in the U.S. between 2005 and 2030	7
1.4 Cumulative revision rate (CRR) of total knee arthroplasties in patients with osteoarthritis (OA) (left) and rheumatoid arthritis (RA) (center) and of unicondylar knee arthroplasties in patients with OA (right)	8
1.5 Risk of first revision following primary TKA by prosthesis type.....	8
1.6 Common revision reasons for TKA and UKA in Swedish Knee Arthroplasty Register 2012	9
1.7 Representative images of the different wear modes defined by McKellop, et al. for hip and knee arthroplasty	11
2.1 Previously published polyethylene damage mode atlas showing characteristic damage modes of the articular surface of polyethylene, a damage mode description and image of typical, visual presentation.....	19
2.2 Damage atlas for metal bearing surfaces, demonstrating characteristic damage modes following in vivo function with associated description and visual presentations acquired using optical stereomicroscopy (12x magnification), interferometry (20-50x magnification), and SEM (50-500x magnification).....	22

List of Figures (Continued)

Figure	Page
2.3 UKA with similar designs to those analyzed in the current study, including (A) Zimmer MG UKA; (B1, B2) Osteonic Single Compartment UKA, a second-generation design that was introduced in 1990 to supersede the Omnifit; (C1, C2) Oxford Mobile-Bearing UKA, with round on flat conformity; and (D) Smith and Nephew Journey UKA, with round on flat conformity.....	30
2.4 Coordinate systems for the femoral and tibial components.....	32
2.5 Distribution of 40 regions equally spaced, covering entire articular surface of femoral component and corresponding zones for analysis.....	34
2.6 UKA femoral component mounted on customized jig and placed on stage of non-contact profilometer, demonstrating ability to control motion in frontal plane (left) and sagittal plane (right).....	35
2.7 Simplified visual of peaks, valleys, and peak-to-valley separations on surface of metallic femoral component.....	36
2.8 Average UKA femoral component surface roughness (Ra) versus in situ time	38
2.9 Average UKA femoral component profile peak height surface roughness (Rpm) and mean maximum profile (Rz) versus in situ time	39
2.10 Representative 3D profilometry surface data of femoral component (left), gross photograph (19 pixels/mm) of femoral and tibial components in anatomical position (center), and polyethylene damage map (right) are shown for the outlying UKA with sever abrasive damage and associated high femoral surface roughness values	39

List of Figures (Continued)

Figure	Page
2.11 Average UKA femoral component surface roughness (Ra) versus total polyethylene damage area. Total polyethylene damage is reported as the surface area damaged as a percent of the total surface area.....	40
2.12 Average UKA femoral component profile peak height (Rpm) and mean maximum profile (Rz) surface roughness versus total polyethylene damage area. Total polyethylene damage is reported as the surface area damaged as a percent of the total surface area	41
3.1 Simplified depiction (left) and photomicrograph (right) of oxidized zirconium alloy	51
3.2 UKA and TKA prostheses analyzed in the current study, including (A) Endosled Waldemar Link UKA from Germany, (B) Johnson & Johnson UKA, (C1, C2) InterMedics Natural Knee, (D) Richards TKA and (E) Smith & Nephew Genesis II	55
3.3 Distribution of 40 regions equally spaced across each condyle of TKA femoral component and corresponding zones for analysis	58
3.4 TKA femoral component mounted in aluminum block on customized jig and placed on stage of non-contact profilometer, demonstrating ability to control motion in frontal plane (left) and sagittal plane (right).....	59
3.5 Roughness (Ra) plot of both TKA condyles where the lateral (left) experienced polyethylene wear through and the medial (right) condyle did not. Red indicates a Ra value greater than 120nm, pink indicates values between 81 and 120nm, yellow indicates values between 51 and 80nm, and cyan indicates values between 21 and 50nm	62

List of Figures (Continued)

Figure	Page
3.6 Gross image (left) and stereomicroscope image at 6x magnification (right) of gross removal of articular surface on Oxinium TKA femoral component	63
3.7 Bearing couple material, SEM images (50-500x) of the area of interest and EDS elemental composition of the corresponding areas for each TKA and UKA of the present study	65
4.1 Historical incidence (1993-2006) and proposed projections of revision total knee arthroplasty in the U.S. The dotted lines represent the 95% confidence interval for the projections from the study	73
4.2 Representative images of tibial components that incorporate a pegged-only design (left) and those that incorporate both pegs and a central stem (right).....	77
4.3 Gross photographs of each individual component of Profix TKA (left) and assembled tibial component With stem of current study (right)	80
4.4 Radiograph with Profix Total Knee System (left) and Natural Knee (right).....	81
5.1 Archard's wear law	87
5.2 Description of different scales to consider when characterizing contact between two bearing surfaces in TKA	89
5.3 Simplified cartoon demonstrating real contact area between two bodies in contact	90
5.4 Representative image of point (left) and line (right) contact determined by shape and conformity of bearing surfaces	91

List of Figures (Continued)

Figure	Page
5.5 Tibial plateau stress versus contact area for different daily activities for a 70kg female. Uniform stress distribution is assumed. The horizontal bar indicates the yield range of polyethylene while the vertical bars demonstrate the range of tibiofemoral contact area of tested knee prostheses (TK), a knee joint after menisectomy (MK) and a natural knee joint (NK)	93

CHAPTER ONE

INTRODUCTION

Knee Arthroplasty

Joint arthroplasty is an orthopaedic surgical procedure used to treat degenerative or inflammatory arthritis and other pathologies affecting the joints. Typical clinical indications for this type of procedure include, osteoarthritis, rheumatoid arthritis, and post-traumatic osteoarthritis. Joint arthroplasty successfully restores joint function by removing the painful arthritic joint surfaces and replacing them with metal alloys, ceramics, or polymeric prosthesis components. The first time these procedures are performed on a joint, they are termed primary, whereas, revision surgeries require the removal of the primary, failed prosthesis and replacement with a new prosthesis.

Knee arthroplasty typically involves the replacement of the surfaces of the tibia, femur and patellar bones. The femoral components and tibial baseplates of total knee arthroplasties are typically made of a cobalt-chrome alloy (ASTM F75) or titanium alloy (ASTM F1108 or F1472). The tibial insert and patellar button are commonly made of ultra-high molecular weight polyethylene (ASTM F648). A new material being used for femoral components is zirconium, which is a metal that can be oxidized to create a ceramic oxidized zirconium surface. Components are being manufactured such that they consist of a zirconium-niobium (Zr-2.5Nb) alloy core (ASTM F2384) and a ceramic, zirconia (ZrO₂) articulating surface. [44] A table comparing the properties of typical materials used in joint arthroplasties is included in Chapter 3 (Table 3.1).

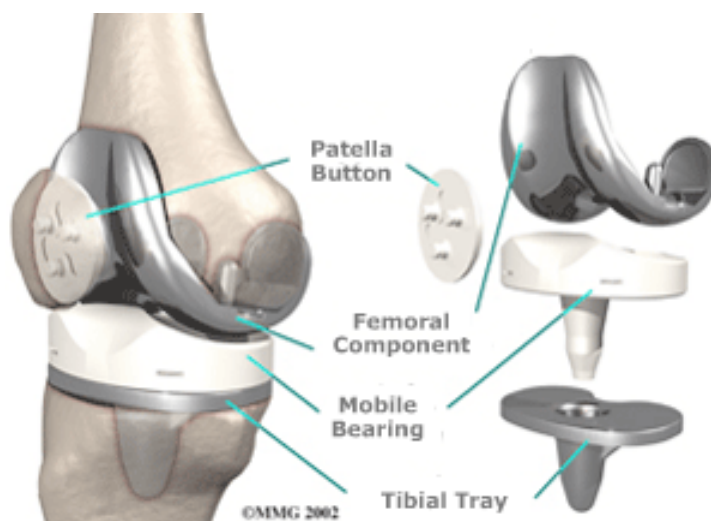


Figure 1.1: Typical total knee arthroplasty components [13]

Typical design considerations of knee replacement prostheses focus on kinematics (i.e. range of motion allowable by the prosthesis) and kinetics (i.e. amount and location of forces the prosthesis is capable of withstanding). The geometry and articulations of the knee are highly complex and include flexion and extension in the sagittal plane, with additional femoral external rotation and roll back occurring during flexion. These motions subject knee prostheses to forces of compression, tension, axial torque, varus/valgus movements, and shear. [83] Knee joint flexion ranges from 0° to 70° during gait, [76] 0° to 90° during stair climbing or sitting, and 20° to 115° during less frequent activities such as kneeling or squatting. [71] Joint loads experienced by the knee, as a function of body weight, vary considerably during different activities, ranging from approximately 2.5 times body weight for gait, as well as kneeling or squatting [29, 71] to 3.5 times body weight for stair ascent/descent [71] to up to 4.5 times body weight for jogging. [29] The average anatomic alignment of the knee is 7° - 10° valgus; however, the mechanical axis of loading passes medial on the knee during stance, leading to a greater

medial load due to varus thrust during gait. [29] Contact stresses of knee replacements differ with conformity of the polyethylene surface, but are generally between 40 and 60 MPa. [17] Typical sliding contact distances of the articular bearing surfaces have been reported to be approximately 20.8-20.1 mm per gait cycle. [33] Assuming a person completes about 1 million cycles per year, this leads to a sliding distance of around 20 km per year for the bearing couple. [33]

Knee arthroplasties can either be performed as a unicondylar (or unicompartamental) knee replacement (UKA) or total knee replacement (TKA), depending on the severity and location of the joint pathology, as well as activity level of the patient. Unicondylar knee replacement involves the restoration of only one condyle of the femur and tibia, either the medial or lateral, without disruption of the surrounding ligaments; whereas, TKA involves resurfacing both condyles and the possible removal of the posterior cruciate ligament. These are discussed later in further detail.

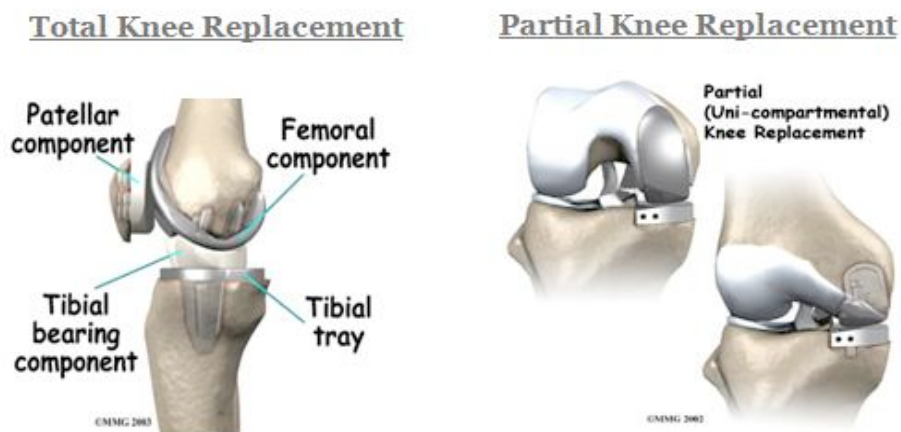


Figure 1.2: Image demonstrating difference between TKA and UKA [87]

The femoral and tibial baseplates of knee replacement prostheses can be manufactured to allow the components to be press-fit or cemented to the bones, once they are surgically prepared. Typically, this decision depends on the quality of the surrounding bone, in that severely damaged or osteoporotic bone may prevent substantial bone in-growth to the press-fit prosthesis, causing instability and loosening. Following revision surgery with significant bone loss, prostheses must be cemented to fill the void and ensure stability. Alternatively, in severe cases, bone grafts and augments, such as stems and wedges, are utilized.

Knee replacement prostheses can be designed as mobile or fixed bearing, depending on the desired range of motion. Mobile bearing prostheses allow the polyethylene tibial insert to move relative to the tibial baseplate. Conversely, fixed bearing prostheses have the tibial insert attached to the baseplate such that relative motion between the components is not possible. Mobile bearing designs have highly conforming tibial inserts and allow for both rotation and translation during weight bearing. [73] In addition, they have been shown to demonstrate reduced volumetric wear. [44]

In addition, tibial components can be composed of all polyethylene or have an articulating surface of polyethylene backed with metal. Metal-backed, modular tibial inserts improve fixation of the tibial component and decreases the stress experienced by the underlying bone and cement. [16, 44, 68, 73, 83] These designs also allow surgeons to choose from different polyethylene inserts during implantation and give them the option to replace only the tibial insert during revision surgery. [73, 83] The disadvantages

of these designs are the typically thinner polyethylene inserts that must be used, which are often associated with increased wear rates, and greater resectioning of the proximal tibia. [83]

Well-known national joint registers have shown that historical survivorship rates of knee arthroplasties range from 65% to greater than 95%, with marked variations in the cumulative revision rates evident due to differences in knee pathology and improved designs introduced in the past two decades (Figure 1.4). [10]

Unicondylar versus Total Knee Arthroplasty

Unicondylar knee replacement involves the treatment of only one condyle of the knee. UKA are typically used in younger, more active patients and in patients with less severe disease, with potential for better ultimate function due to less joint pathology, but a higher risk of failure and increased wear rates. [74] It has been reported that UKA usually permit for a better preservation of soft tissue and bone stock, a less invasive procedure allowing decreased recovery time, and a better overall function with improved range of motion and more natural gait. [74, 81]

Total knee replacement is the more commonly implanted design and involves the replacement of both condyles of the knee. It is generally performed in older patients and those with more complex knee pathologies. While the procedure is more invasive and destructive to the bone stock, it is often associated with a lower rate of revision. [23] Some studies have shown TKA to result in worse outcomes and greater risk of complication compared to UKA; however, it should be noted that patients who undergo these types of procedures are often being treated for rheumatoid arthritis and other more

complicated pathologies, indicating a more extreme pathological condition to overcome. [23]

There are many varying designs of TKA aimed at being the most representative of physiologic conditions. Cruciate retaining designs allow the motion of the knee to be dictated by the surrounding soft tissues and ligamentous structures, mainly the posterior cruciate ligament (PCL). [73] Posterior stabilized designs are highly conforming and allow for a decrease in load on the surrounding tissues. The design incorporates a post on the tibial insert that fits into a cam in the femoral component, which prevents posterior subluxation of the tibia while maintaining the femur in a posterior position during knee flexion. [73] Some designs also make use of dished polyethylene inserts, which have a raised anterior lip to improve anteroposterior stability. This prevents uncontrolled sliding, and studies have shown these designs experience low wear with few eccentric wear patterns. [73]

Joint registries from various countries and U.S. databases have shown that the volume of joint arthroplasty procedures performed each year has steadily increased over time, with primary total knee arthroplasties (TKA) projected to increase by 673%, from 450,000 in 2005 to 3.48 million procedures in 2030 (Figure 1.3). [60] Not only is the demand for these procedures increasing, but they also are being performed in younger, more physically active and less compliant patients, indicating an increased need to maximize prosthesis survivorship. [22] In addition, revision TKA surgeries are projected to increase by 601%, from 38,300 in 2005 to 268,000 by 2030, [60] which demonstrates

that improvements in prosthesis design and surgical techniques are still necessary and ultimately vital to improving prosthesis longevity.

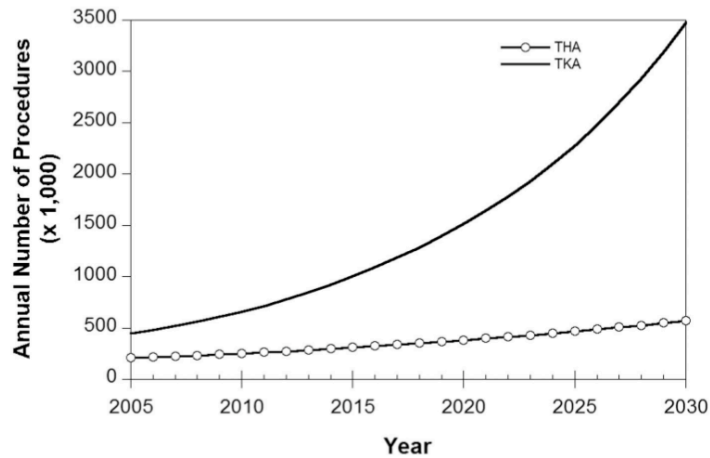


Figure 1.3: Projected number of total knee arthroplasties performed in the U.S. between 2005 and 2030 [60]

Well-known joint registers also report that the risk of revision with TKA has improved with time, except within the most recent portion of the decade (2006-2010). [10] This is especially prevalent in patients receiving treatment for rheumatoid arthritis. Much of the increased risk in the last five years is attributed to the increase in number of revisions due to infection. Conversely, these same registers have shown the risk of revision to stay essentially constant with UKA, which may be caused by a decrease in the number of procedures being performed in the country, as well as a lack of improvement in UKA design. [10] The cumulative revision rates for the Swedish Knee Arthroplasty Register Annual Report 2012 for both TKA and UKA are reported in Figure 1.4. Another register reports the risk of the first revision following primary knee replacement, for any diagnosis, for varying types of TKA and UKA prostheses, which is shown in Figure 1.5

and demonstrates that patello-femoral and UKA had considerably higher rates of revision compared to cemented unconstrained fixed bearing prostheses. [11]

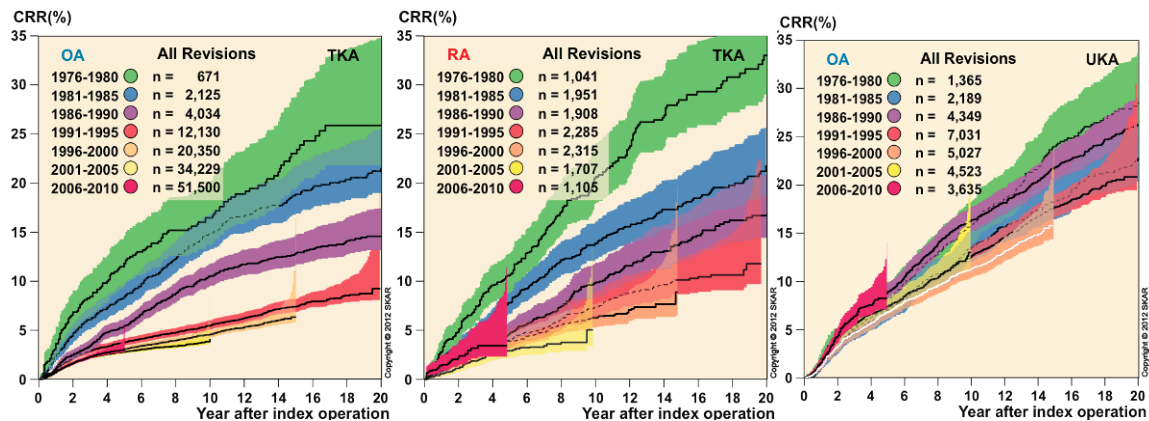


Figure 1.4: Cumulative revision rate (CRR) of total knee arthroplasties in patients with osteoarthritis (OA) (left) and rheumatoid arthritis (RA) (center) and of unicondylar knee arthroplasties in patients with OA (right) [10]

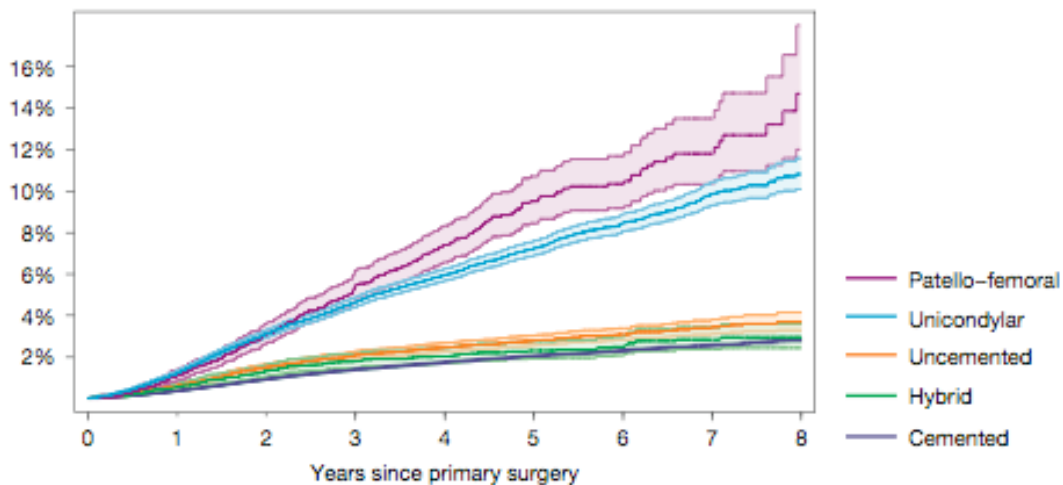


Figure 1.5: Risk of first revision following primary TKA by prosthesis type [11]

There are various reasons, depending on pathology of the patient's joint as well as prosthesis type, which cause the need for revision surgery. Joint registers often report the greatest contributors as being loosening, infection, wear, progression of pathology, and

instability. These reasons are summarized in Figure 1.6 for TKA in patients with osteoarthritis (OA) and rheumatoid arthritis (RA), as well as UKA in patients with OA.

[10]

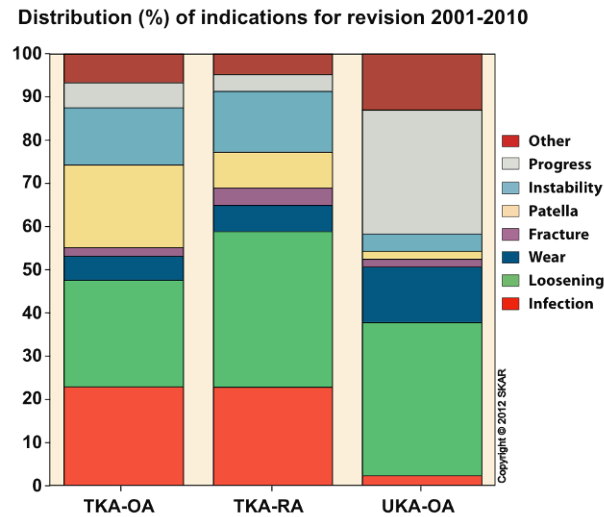


Figure 1.6: Common revision reasons for TKA and UKA in Swedish Knee Arthroplasty Register 2012 [10]

Wear of Arthroplasty Prostheses

While total joint replacement continues to be a successful, cost-effective procedure, there are many studies that demonstrate wear and its sequelae as the major limitation of joint replacement longevity. [14, 57, 70, 73] Studies have shown that wear debris is generated from four main locations, including articulating surfaces, modular component surfaces, fixation surfaces, and fixation augments. [14, 57, 70] In order to better describe these interactions, McKellop, et al. developed the four common modes of wear typically present in total joint replacements. [70] These modes are typically cited for total hip replacements but can be applied to various joint replacements, including knee replacements. Mode I is wear debris generated from motion between the primary bearing

surfaces, which is typically metal on polyethylene. This is the most common mode of wear and accounts for the majority of wear in well-functioning joint replacements. [14, 57, 70] Mode II is wear debris generated by motion between two surfaces not intended to come in contact, which often occurs with complete polyethylene wear through. In the knee, this leads to motion between the femoral component and tibial baseplate. Mode III is third-body wear caused by an unintended particle being caught between two primary bearing surfaces. Finally, mode IV is wear generated by motion between two non-bearing surfaces. Examples of this mode include fretting of the Morse taper or stem-cement fretting. [14]

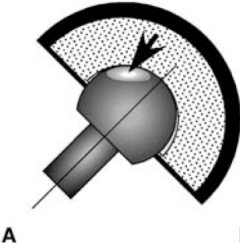
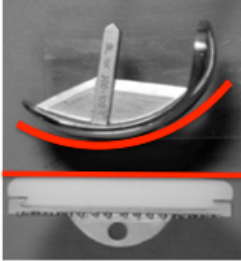
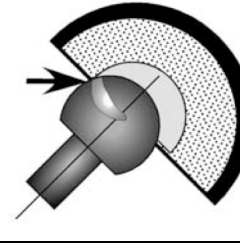
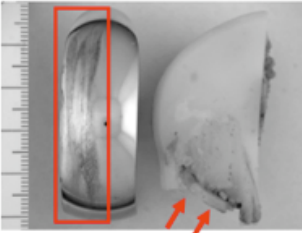

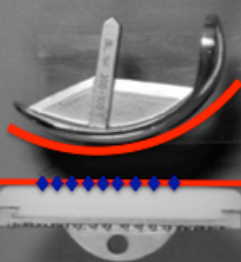
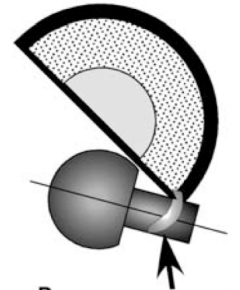
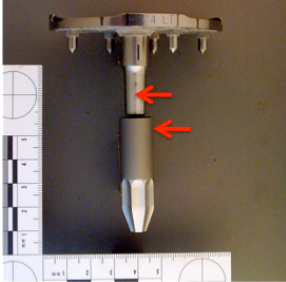
Mode of Wear	McKellop's Representation (Hip)	Representative Image for Knee
Mode I		
Mode II		
Mode III		
Mode IV		

Figure 1.7: Representative images of the different wear modes defined by McKellop, et al. for hip and knee arthroplasty [70]

Wear debris, inclusive of polyethylene, metal, bone and polymethylmethacrylate (PMMA) particulates, is commonly attributed with causing aseptic loosening. [4, 44, 73] In late failure, wear and osteolysis frequently play a prominent role in the cascade to failure; however, failure due to these mechanisms is often cited to occur before 5 years

post-operatively. [4, 73] Failure arises primarily due to the progressive loss of bone stock surrounding the prosthesis, which can cause aseptic loosening, as well as periprosthetic and/or prosthesis fracture. [4, 14, 44, 73] Osteolysis has been found in both cemented and cementless total knee prostheses [14, 44, 57], though the percentage is less for cemented (0-16% versus 6-30%). [44] Additionally, studies investigating periprosthetic membranes of cemented and cementless prostheses with osteolysis suggest that different biological mechanisms led to the loosening that occurs for each type of fixation. [14]

The concentration, size, geometry, and chemistry of the particulate debris influence the host response. [4, 14, 44, 57] For example, larger pieces activate foreign body giant cells, while smaller particulates activate macrophages. [4] It is generally accepted that particles of phagocytosable size elicit a greater immune response and greater concentrations of debris stimulate a larger response. [14, 57] The loss of bone is mediated by macrophages, which are activated by the particulate debris. [4, 44, 73] Macrophages can cause bone resorption indirectly by releasing osteoclast-activating factors, like tumor necrosis factor alpha (TNF- α), or directly by releasing hydrogen peroxide and oxide radicals. [4] Macrophages also are known to synthesize the cytokine interleukin-1 (IL-1), which is proinflammatory and causes both stimulation of osteoclasts and decreased function of osteoblasts. [4, 44]

The predominant particle found in the periprosthetic tissue of total joint replacements is polyethylene. [14, 57, 73] At five years after primary TKA, osteolysis due to polyethylene wear has been cited as the greatest cause for revision surgery. [44] Polyethylene wear debris is typically of the spheroid shape, though fibrillar and globular

forms also have been found. [14, 57] The average size of the debris is about 0.5 μ m, with over 90% of debris particulates being less than 1 μ m in size. [14, 57] Polyethylene wear in knee replacements has been linked to three main types of factors, including patient, prosthesis design, and surgical factors. Patient factors include size and age, which determine the loading conditions, and activity level, which has been shown to increase wear debris generation as it increases. [4, 44, 73] As the age of the patient decreases by 1 year, the chances of experiencing wear-related failure increases by almost 5%, which may be related to patient activity level. [44] Surgical techniques should ensure proper alignment and a balance of loading on ligaments, as poor technique in either area can lead to an uneven distributions of forces and early degradation. [73]

In general, the material combination, quality, surface finish, sphericity and tolerancing of the prosthesis components can influence the amount of debris produced. Specifically for metal on polyethylene combinations, the prosthesis design factors include the polyethylene polymerization process, method of manufacturing, method of sterilization, and polyethylene thickness. [44, 73] Flaws, such as cracks or voids, introduced during the polymerization process can lead to delamination or crack propagation, and studies have shown that compression molded polyethylene inserts wear less than those machined from ram-extruded stock. [44, 73] Presently, inserts are generally sterilized in ethylene oxide or undergo gamma radiation without the presence oxygen. This has changed from previous methods with the understanding that gamma radiation in air introduced free radicals into the material, which later underwent oxidation, causing the rapid degradation of the material. [73] Bartel, et al, showed that

contact stresses increased exponentially as polyethylene thickness decreased and that a thickness of at least 8mm allowed for a more even distribution of contact stress across the surface, which has now become the generally recommended insert thickness. [17, 44, 73]

The articular surface of the polyethylene also can influence the generation of wear debris. Designs generally aim to decrease contact stress and loading in order to increase wear resistance. [73] In general, conformity is defined by the radius of the femoral and tibial component, with the radius of the tibia always being larger than that of the femur. While less conformity between the femoral component and tibial insert mimics physiologic conditions, making the geometry of the prosthesis more conforming increases the contact area, which decreases the contact pressure and stresses. [44, 73] However, since higher conformity generates shear stresses and often creates torque about the long axes of the femoral and tibial component, it may increase the stresses experienced at the component-bone interface. [44, 73]

Although similar wear modes are present in both total knee and total hip replacements, wear mechanisms of the knee vary widely from those experienced by the hip. [14, 44, 73] The articulations of the knee and its geometry are very complex and are thus, very difficult to mimic. The knee joint undergoes rolling, sliding and rotation, introducing a multitude of mechanisms through which the polyethylene can be expected to wear. Studies have shown that the predominant mode of polyethylene failure in knees is due to fatigue, producing large, irregular-shaped particles, whereas in hips, the predominant mode is abrasive and adhesive wear, leading to much smaller particles that increase the host response. [14, 44]

Metal debris also plays an important role in biological activity resulting from wear debris production. The type of metal particulates greatly influences the host response. [44] Titanium has been shown to be minimally toxic to macrophages; however, it has a greater stimulatory effect on the proinflammatory mediators, such as IL-1. [14, 44] Conversely, cobalt-chromium is extremely toxic to macrophages and causes an early death, which diminishes the effects of the mediators. [14, 44]

Wear remains as a one of the most important concerns in joint replacement due to its influence on osteolysis, aseptic loosening, and ultimately revision. Wear debris generated by mode I, II, and IV wear can further lead to third-body wear (mode III) by allowing the debris to enter the joint space. [4] Debris can gain access to all areas in the joint and surrounding tissues that joint fluid can access. [14] This debris ingress into the periprosthetic space often occurs through screw holes or along radiolucent lines. The end result of wear-activated macrophage activity is typically loss of bone, osteolytic lesions, granulomatous lesions, also known as pseudotumors, or prosthetic synovitis.[4]

Purpose

While total joint replacement continues to be a successful treatment for degenerative joint disease, there are many studies that demonstrate wear and its sequelae as the major limitation of joint replacement longevity. Previous studies have shown that wear debris originates from four main locations: articulating surfaces, modular component surfaces, surfaces of fixation, and adjuvant fixation devices. [14, 57, 70] Each of these possible wear sources can initiate the cascade of failure associated with wear-induced osteolysis and lead to subsequent revision surgery. The objective of this thesis is

to characterize the *in vivo* performance of knee prostheses by quantitatively assessing performance at different potential wear-inducing interactions, including bearing surfaces and modular augments. The objective will be accomplished through three studies that will aim to investigate wear modes I, II, and IV.

The purpose of Study 1 is to explore the relationships between femoral component surface roughness, polyethylene insert damage and *in vivo* duration through the evaluation of metal-polymer UKA bearing couples that were retrieved after 1 to 19 years of *in vivo* service. This study characterizes the distribution of damage on matched metal-polymer bearing couples of retrieved UKA and quantify ranges of surface roughness corresponding to the different damage modes visually identified on both bearing surfaces. The purpose of Study 2 is to characterize the damage of retrieved knee replacement bearing couples that have experienced complete polyethylene wear-through, while considering the material properties of the metal alloys. The purpose of Study 3 is to evaluate the clinical outcomes of 84 patients implanted with primary TKA prostheses of a single design, which utilizes a Morse taper design feature for attaching a modular tibial stem.

CHAPTER TWO



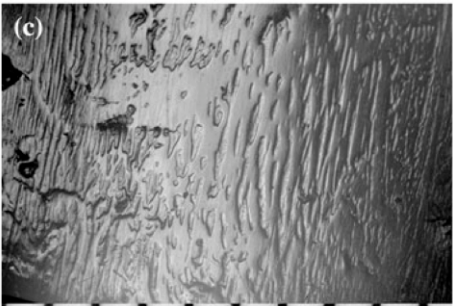

STUDY 1: MODE I WEAR

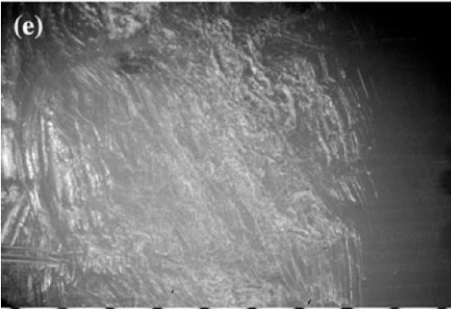
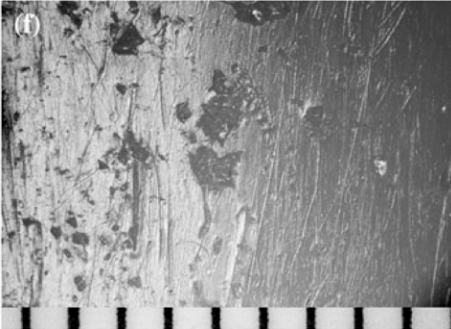
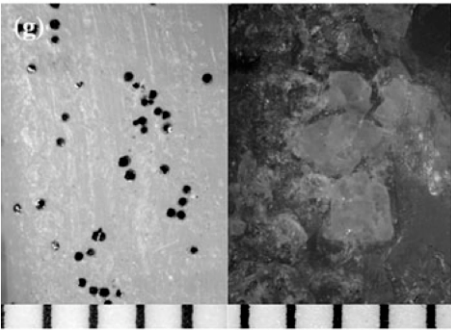
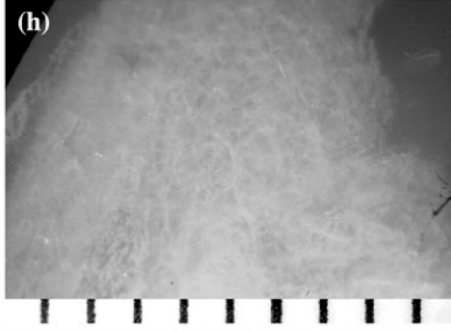
Introduction

Mode I wear results from the articulation between two primary bearing surfaces, as intended by the designer. It typically generates the greatest amount of debris and is often considered the most important mechanism leading to prosthesis failure. [14, 18, 70] Polyethylene wear is dependent on a multitude of factors, including surgical techniques, design-related, and biomaterial properties and processing techniques of both the femoral component and tibial component.

Wear occurring at the bearing surfaces of knee replacements is typically caused by the intended articulation of a metallic or ceramic femoral component and polyethylene tibial insert. The predominant modes of wear particle generation that occur at the bearing surface consist of pitting, surface delamination, and adhesive and abrasive wear of the polyethylene, with delamination remaining the cause of most primary TKA failures. [44] Delamination occurs when the polyethylene experiences fatigue following repetitive stress, causing the initiation and propagation of cracks beneath the surface. [44] This results in large flakes, typically greater than 5mm, being removed from the surface. [44] Adhesive wear results in the removal of small particulates, generally several microns in size. [44] Abrasion is caused by asperities on the femoral component or third-body particles, harder than the polyethylene, cutting and removing particulates from the articular surface of the softer polyethylene. [44]

Polyethylene damage modes are well defined in the literature. [47] Wear can occur on both the articulating surface of the tibial insert, as well as the backside of metal-backed designs, where the polyethylene contacts the underlying tibial baseplate. Since the focus of the present study is on bearing surface wear debris generation, backside damage modes are not presented. Figure 2.1 defines the ten common damage modes of polyethylene (non-articular deformation, burnishing, striations, scratches, abrasion, pitting, embedded debris, subsurface cracking, delamination, and fracture) and demonstrates their common visual presentation on retrieved prostheses.

Damage Mode	Description	Visual Image
Non-articular Deformation	Permanent change in shape not associated with condylar articulation	
Burnishing	Smooth, highly polished regions highly reflective of light	
Striations	Highly oriented, longitudinal or dispersed, smooth peaks and troughs	
Scratches	Thin lines in irregular or ordered directions	

Abrasion	Rough, tufted regions with limited directionality	
Pitting	Depressions with rough surfaces and a typical diameter between <math><1\text{mm}</math> and 2mm or greater	
Embedded Debris	Particles that differ in color and/or texture relative to surrounding polyethylene surface, consistent with third-body particles of bone, cement fragments or metal	
Subsurface Cracking	Cracks and/or discoloration located inferior to the articular plane without surface discontinuity or rupture	

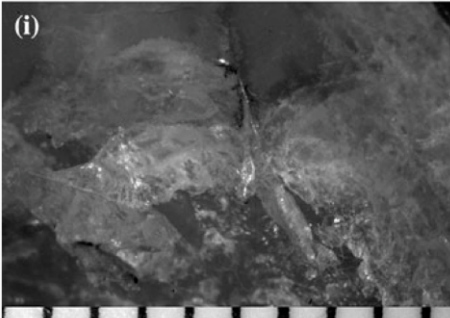
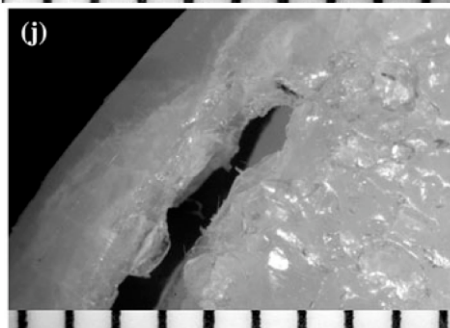
Delamination	Visualized as thin layers of polyethylene material separated from the surface, with the remaining exposed material typically appearing textured and/or grossly pitted	
Fracture	Complete cracks or wear-through of the polyethylene bearing, typically resulting in exposure of the metal baseplate or discontinuity of the bearing rim	

Figure 2.1: Previously published polyethylene damage mode atlas showing characteristic damage modes of the articular surface of polyethylene, a damage mode descriptions, and images of typical, visual presentation [47]

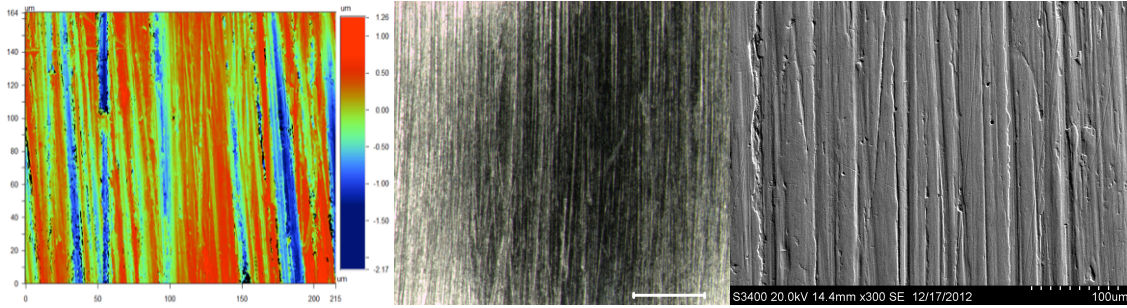
Since metallic surface damage modes vary in both their presentation and mechanism compared to polyethylene damage, it has been necessary to clearly define these metallic damage modes. [3] While oxidized zirconium alloy has a ceramic-like articulating surface, it is believed to experience similar damage modes as those visualized on purely metallic components. Each of the eight common damage modes (abrasion, dulling, material transfer, pitting, scratching, dimensional changes, removal marks, fracture) used to assess the retrieved knee prostheses of the present studies are summarized in Figure 2.2, including both descriptions and various visual aids.

Damage Description and Visual Images acquired using Optical Stereomicroscope (12x magnification) (left), Interferometer (20-50x magnification) (center) and SEM (50-500x magnification) (right)

Damage Mode

Abrasion

Scraping and roughening of surface due to presence of high hardness particles producing random array of fine, shallow scratches



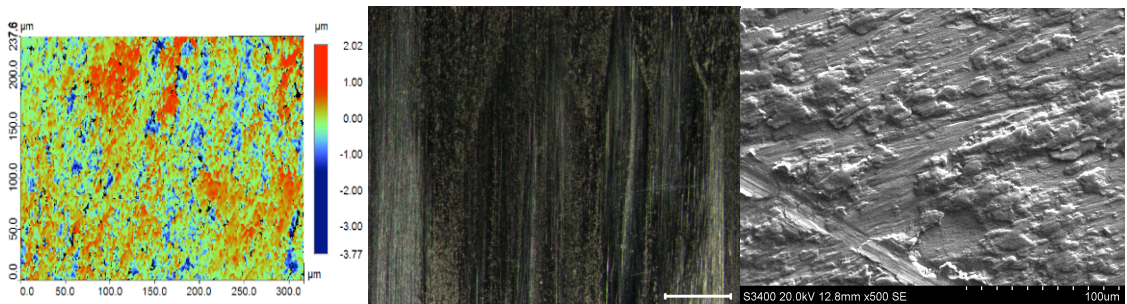
Dulling

Abrasive wearing of surface to produce matted, discolored appearance



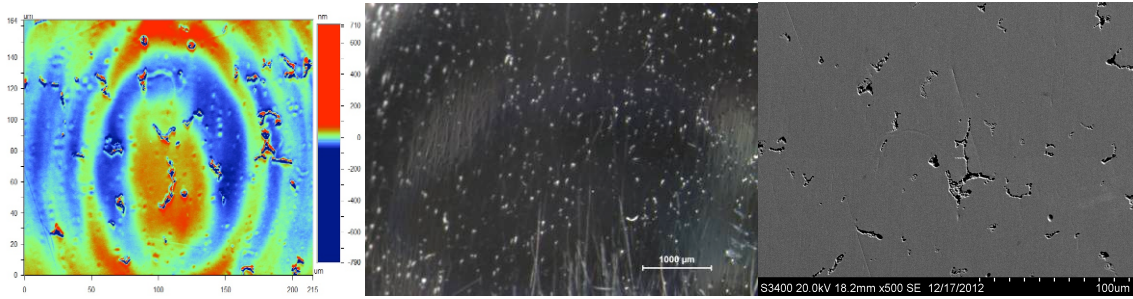
Material Transfer

Localized material transfer or formation of surface protrusions caused by two solid surfaces sliding under load



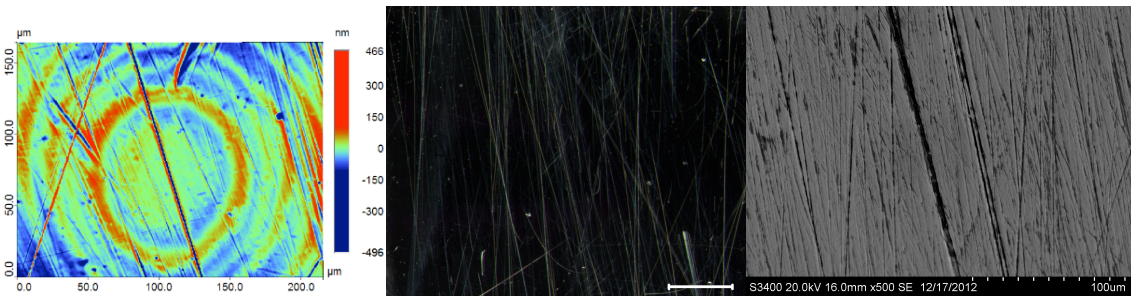
Pitting

Irregular or circular shaped craters produced due to localized fatigue failure



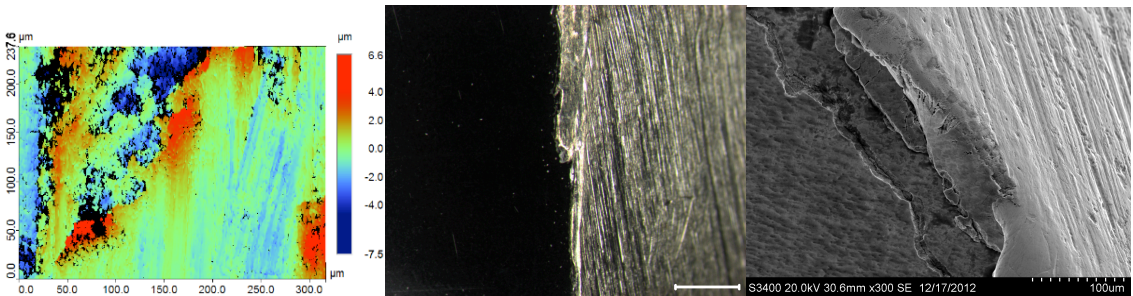
Scratching

Motion directed surface removal or displacement of material due to presence of foreign abrasive particles or protrusions



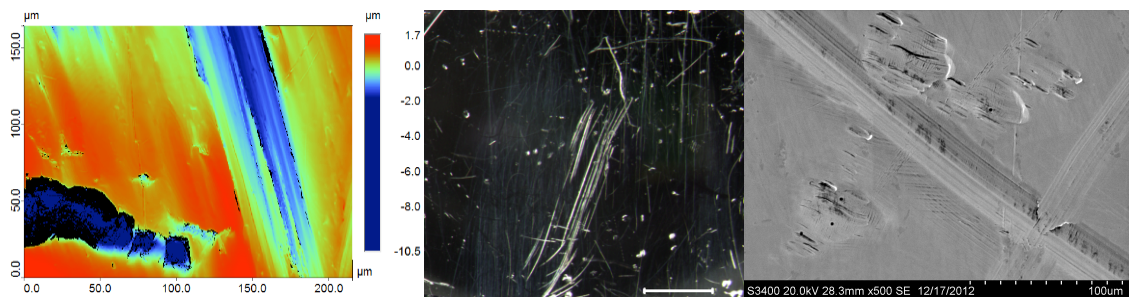
Dimensional Changes

Macroscopic surface removal caused by two solid surfaces sliding under load



Removal Marks

Irregular, sharp, distinct, deep scratches produced by surgical tool



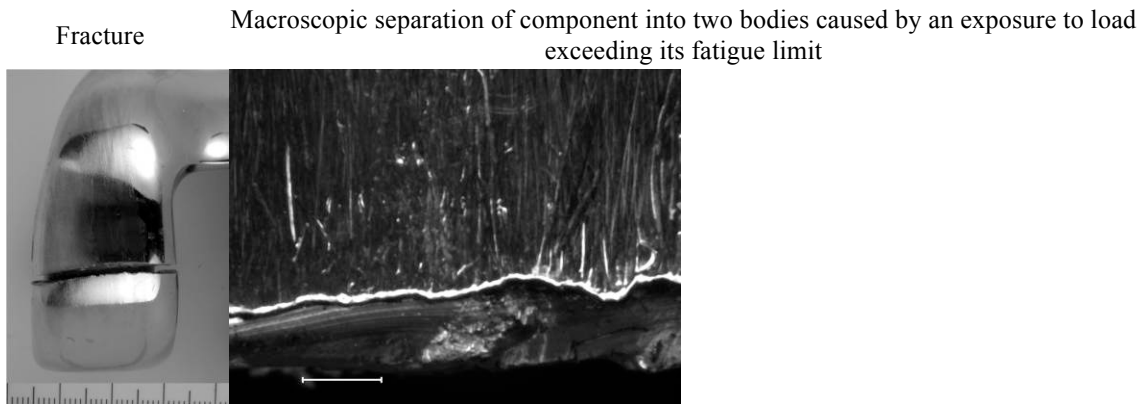


Figure 2.2: Damage atlas for metal bearing surfaces, demonstrating characteristic damage modes following in vivo function with associated description and visual presentations acquired using optical stereomicroscopy (12x magnification), interferometry (20-50x magnification), and SEM (50-500x magnification). [3]

The material properties and surface topography of both the polyethylene insert and the metal femoral component play a crucial role in subsequent wear processes. [28, 35, 80] The roughness of the femoral component can affect articulating surface frictional coefficients and modes of bearing lubrication. [1, 34] During in vitro wear simulation, metal femoral components can experience an increase in surface roughening, and this additional roughening usually determines both polyethylene wear volume and number of particles produced. [39] However, this relationship is not well established for knee prostheses retrieved after in vivo function. During functional use in patients, roughening of the metal femoral component can be caused by the presence of third body materials, such as bone, bone cement, or metal particles, between the articulating surfaces of the joint (mode III wear). [39, 78, 80] Thus, it is important to consider both the initial roughness of the femoral component, as well as other effects that may contribute to prosthesis wear that occurs during functional loading. [34] Moreover, the types of damage modes on the polyethylene bearings that are present after in vivo loading can

vary considerably from those observed after in vitro simulation. [48, 51] Previously, Harman, et al. [48, 52] used retrieved UKA to demonstrate the distribution of damage modes and damage sizes that occur after in vivo function. In those studies, characteristic damage modes (Figure 2.2) were linked to prosthesis alignment and loosening, but assessments of the bearing couple were not completed. Therefore, the role of femoral component surface roughness was not considered as a factor in the observed damage on those polyethylene inserts.

Advances in TKA are meant to improve longevity by limiting polyethylene wear. Studies have shown that joint replacement, in general, tend to wear more quickly during in vivo service than predicted by controlled laboratory tests [35, 80] Moreover, the types of damage modes on the polyethylene bearings that are present after in vivo loading can vary considerably from those observed after in vitro simulation. [48, 51] While several advancements made in joint replacement have been focused on making the surface of the polyethylene insert more resistant to wear, through variations in the sterilization and manufacturing processes, many also have attempted to make the articulating surface of the femoral component harder, smoother and more damage resistant. Early knee arthroplasties utilized titanium alloys for both the femoral and tibial components because it was thought that they would provide the necessary biocompatibility and strength needed for these components. Consequently, cobalt-chrome alloys began to be used because their increased hardness and decreased surface roughness achieved during manufacturing. This material is the most commonly used material today for femoral components because it provides the strength and hardness necessary to withstand

physiologic loading conditions. Newer, ceramic-like materials, such as oxidized zirconium, are being explored due to their increased hardness and smoothness, as well as the corrosion and scratch resistance that they provide.

In an attempt to make wear simulations more predictive of wear volume, wear rate and damage modes observed during in vivo function, some studies report methods for inducing damage on the metal femoral component prior to testing. DesJardins, et al. simulated in vivo function by obtaining four brand new femoral components and subjecting them to equal roughening treatments, in which they were tumbled with 25 μ m alumina powder and plastic cone media in a centrifugal finishing barrel for 30 seconds. [34] Similarly, Muratoglu, et al. selected the five femoral components with the most visual third body damage from a group of retrieved prostheses, obtained roughness measurements from a limited number of selected regions on the contact surface of each, and chose the four prostheses with the highest roughness values to use in the simulation study. [72] While these studies of simulated gait activity each show that femoral components having higher surface roughness can increase the associated polyethylene wear rate compared to new components, it remains unclear whether in vivo function of knee replacements results in the same magnitude of increased roughness and polyethylene wear. Moreover, given that scratches typically are oriented along the direction of knee flexion and antero-posterior sliding, it is not clear that diverse scratch orientation resulting from tumbled roughening is representative of in vivo conditions.

Previous studies have shown that volumetric wear of polyethylene is determined by several factors, including applied load, sliding distance, and a wear factor, which is an

exponential function of measured surface roughness, particularly R_a . [35] Thus, measures of increased roughness of metal counter-bearing surfaces can predict increases in polyethylene wear. [32, 35, 65] Some studies have shown that a threefold increase in femoral component surface roughness can lead to a minimum tenfold increase in the polyethylene insert wear rate. [64] However, it remains unclear whether in vivo function increases metal bearing surface roughness with an associated increase in polyethylene wear. Previous studies by Alvarez, et al. [2] and Harman, et al. [52] established standardized methodologies for assessing the entire articular surfaces of retrieved UKA femoral components and tibial inserts. Based on a small group of retrieved UKA, there was a significant correlation between surface roughness and polyethylene damage area. [2] However, those studies [2, 52] included only one UKA design from a single manufacturer with a limited range of in vivo duration.

The purpose of the current study was to explore the relationship between femoral component surface roughness, polyethylene insert damage and in vivo duration through the evaluation of metal-polymer UKA bearing couples that were retrieved after 1 to 19 years of in vivo service. This study aimed to characterize the distribution of damage on matched metal-polymer bearing couples of retrieved UKA and quantify ranges of surface roughness corresponding to the different damage modes visually identified on both bearing surfaces. Two hypotheses were considered based on previous work completed by Alvarez et al. [2] and Harman et al. [52]. First, it was hypothesized that the magnitude of femoral component surface roughness would increase with longer duration of function.

Second, it was hypothesized that increased metal bearing surface roughness would correlate with greater areas of polyethylene damage.

Materials and Methods

Twenty-nine UKA were retrieved during revision arthroplasty at three institutions located in the United States (Good Samaritan Medical Center, West Palm Beach, Florida; Palm Beach Gardens Medical Center, Palm Beach Gardens, Florida) and Germany (University Hospital Mannheim, University of Heidelberg, Mannheim, Germany) over a sixteen-year period (1994-2010). The components were retrieved for reasons typical for clinical outcomes in UKA, including aseptic loosening (7), polyethylene wear (2), progressive arthritis (3), pain and instability (2), and for unknown reasons. These UKA were archived in an established, institutional review board approved Implant Retrieval Program in operation since 1992. [49] The entire bearing couple (femoral component and tibial polyethylene insert) was available for 22 UKA in this cohort, with 3 couples experiencing complete polyethylene wear-through leading to metal-on-metal contact between the femoral component and tibial baseplate. These 3 specimens were excluded from our study, as they represent a cascade of failure that was not consistent with only metal-on-polyethylene mode I wear. The remaining 19 UKA bearing couples are the focus of this study. Surgical technique included implantation in the medial compartment in 18 knees and in the lateral compartment in 1 knee. Cement fixation was used for 19 femoral components and 18 tibial components, whereas uncemented fixation was used in 1 tibial component. Sixteen of the tibial inserts were metal-backed, while the remaining 3 were all polyethylene tibial components. All UKA had non-conforming tibio-femoral

articulations with fixed-bearing polyethylene inserts and included designs fabricated by 6 different manufacturers (Table 2.1).

Prosthesis #	Manufacturer	Conformity*	Tibial Base Plate**	Bearing	Fixation	Implantation Site
K2099_96L	Zimmer	ROF	MB	Fixed	Cemented	Lateral
K1120_96R	Richards	ROF	MB	Fixed	Cemented	Medial
K2001_97R	DePuy	Flat	MB	Fixed	Cemented	Medial
K2002_97L	Richards	ROF	AP	N/A	Cemented	Medial
K2131_97R	Osteonics	ROC	MB	Fixed	Cemented	Medial
K2097_98R	Zimmer	ROF	MB	Fixed	Cemented	Medial
K2089_01R	Richards	ROF	MB	Fixed	Uncemented	Medial
K1025_02L	Unknown	ROF	AP	N/A	Cemented	Medial
K2067_02L	Zimmer	ROF	MB	Fixed	Uncemented	Medial
K1016_03L	Unknown	ROC	MB	Fixed	Uncemented	Medial
K2017_04R	Link	ROF	MB	Fixed	Cemented	Medial
K2018_04L	Link	ROF	MB	Fixed	Cemented	Medial
K2028_04R	Link	ROF	MB	Fixed	Cemented	Medial
K2042_04R	Link	ROF	MB	Fixed	Cemented	Medial
K2043_04R	Link	ROF	MB	Fixed	Cemented	Medial
K2044_04L	Link	ROF	MB	Fixed	Cemented	Medial
K2093_05L	Link	ROF	MB	Fixed	Cemented	Medial
K2040_04L	Endoplus	ROF	MB	Fixed	Cemented	Medial
K2001_10L	Link	ROF	MB	Fixed	Cemented	Medial

*Conformity defined as round-on-flat (ROF) or round-on-curved (ROC)

**Tibial baseplate design defined as metal-backed (MB) or all polyethylene (AP)

Table 2.1: Available data on retrieved unicondylar knee prostheses.

At this time, the polyethylene materials (ram-extruded or compression molded) and sterilization methods (gamma radiation or ethylene oxide) could not be determined for all prosthesis designs, since the original packaging labels were not available. Figure 2.3 demonstrates several UKA designs similar to those analyzed in the current study, including several with a round-on-flat articulating design. For the purposes of this study, round-on-flat (ROF) is defined by a tibial component having an infinite radius.

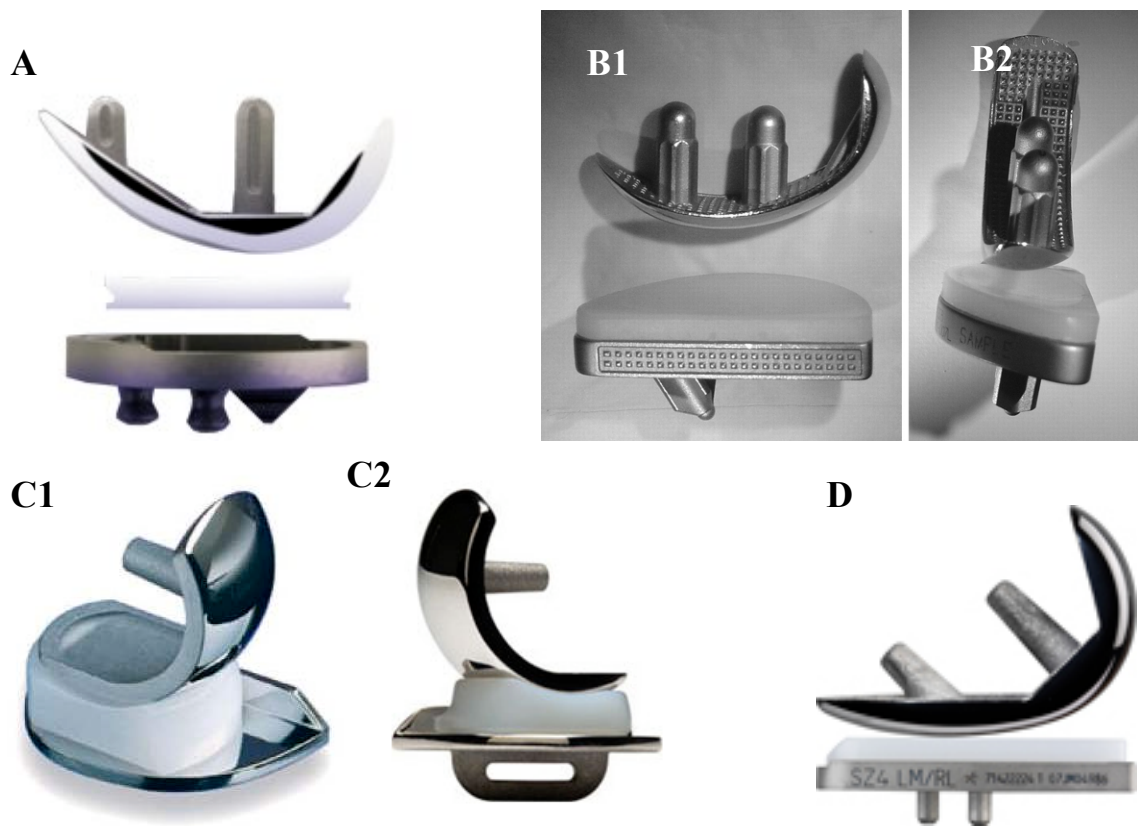


Figure 2.3: UKA with similar designs to those analyzed in the current study, including (A) Zimmer MG UKA; (B1, B2) Osteonic Single Compartment UKA, a second-generation design that was introduced in 1990 to supersede the Omnifit [26]; (C1, C2) Oxford Mobile-Bearing UKA, with round on flat conformity; and (D) Smith and Nephew Journey UKA, with round on flat conformity

Patient demographics were obtained from available medical records. Included in this study were 11 female and 8 male patients with a mean age of 70.7 (SD 6.0, range 61.9-81.7) years at index surgery and mean age of 71.1 (SD 12.1, range 45.0-84.8) years at the time of retrieval. Nine of the prostheses were implanted in the right knee and ten in the left. Average duration of in vivo function for these prostheses was 88.1 (SD 60.7, range 10.0-224.0) months. Additional patient data were available from some surgeons, but not others, as summarized in Table 2.2.

Prosthesis #	Sex	Age at Index	Age at Retrieval	Time In situ (mos.)	Weight (kg)	Height (cm)	Revision Reason
K2099_96L	M	44.2	45.0	10.0			pain, ACL deficient
K1120_96R	M	70.0	81.9	144.0			loose tibia, PE wear
K2001_97R	M		63.0				
K2002_97L	M	66.0	82.2	224.0			loose tibia, PE wear
K2131_97R	F		63.0				PE wear
K2097_98R	M	78.0	84.8	90.0			pain, instability
K2089_01R	M	52	65.0	156.0			PE wear
K1025_02L	M	50.8	54.0	38.0			loose tibia
K2067_02L	M						
K1016_03L	F		53.0	18.2			
K2017_04R	F	63.5	76.5	156.3	65	162	patellar OA
K2018_04L	F	61.9	67.5	67.2	85	158	aseptic loosening
K2028_04R	F	81.7	83.7	24.7	71	155	aseptic loosening
K2042_04R	F	76.0	84.3	99.4	90	155	
K2043_04R	F	70.3	76.4	72.8	99	162	patellar OA
K2044_04L	F	68.2	76.4	99.3	87	168	progressive OA
K2093_05L	F	67.1	68.2	14.1	68	164	loosening
K2040_04L	F				90	170	loosening
K2001_10L	F	74.8	83.8	108.4			
Average		70.7	71.1	88.1	83	161	
SD		6.0	12.1	60.7	11	6.0	

Table 2.2: Available clinical data for patient population

All retrieved components were handled similarly, following protocols established at the retrieval lab, including fixation in formalin, cleaning using a mild detergent and a nylon brush, followed by sonication, rinsing in clean water and ethanol, and air drying. A component-based coordinate system was established for the bearing surfaces of the femoral component and tibial component using reference features that were consistent across the included UKA designs and overall dimensions of each component (Figure 2.4).

For the tibial components, the reference features included the flat intracondylar side and the anterior and posterior rim of the insert, as previously described by Harman, et al. [52] Thus, the tibial damage patterns were measured in a grid covering the entire bearing surface that was defined relative to the anterior-posterior and medial-lateral periphery of the articular surface.

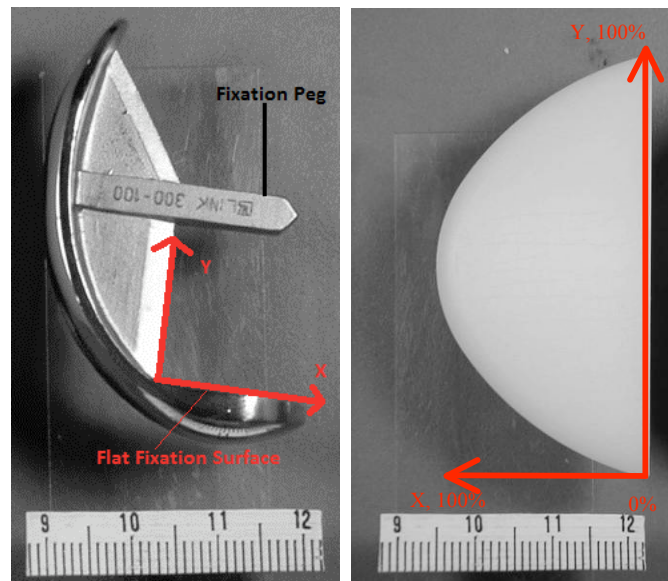


Figure 2.4: Coordinate systems for the femoral and tibial components

Damage on the articular surface of the polyethylene tibial inserts was visually assessed using an optical stereomicroscope (model Z30L, Cambridge Instruments, Cambridge, Massachusetts) with lenses providing magnification of 7x to 26x and an illustrative polyethylene damage mode atlas. [47] According to this atlas, ten characteristic polyethylene damage modes (non-articular deformation, burnishing, striations, scratches, abrasion, pits, embedded debris, subsurface cracking, delamination, and fracture) were visually assessed (Figure 2.1).

As previously described in a published study, [52] calibrated digital images were measured to determine the damage area relative to the insert's bearing surface area. To briefly explain the methodology of this published study, damage area was defined as the percentage of total articular surface damage, measured using photogrammetry techniques applied to calibrated digital images. The magnitude of linear surface deformation was evaluated using a contact point digitizer (Microscribe 3DX, Immersion Corp., San Jose, California). Deformation rate was calculated as maximum linear deformation divided by duration of function.

For the femoral components, the reference features included the fixation pegs, the flat fixation surface for the posterior condyle and the anterior and posterior condylar rims. The overall width and length of the articular surface of each individual femoral component was measured using a flexible ruler, subtracting 10% of the total length and 5% of the total width to accommodate small shape deviations, since the bearing surface was not an exact rectangle. These dimensions were used to define a uniform 3-dimensional grid of 40 regions equally spaced across the entire articular surface of each femoral component (Figure 2.5). This distribution of 40 points across the articular surface of each implant design led to an approximate point spacing of 8-10mm anterior-posteriorly and 3-6mm medial-laterally.

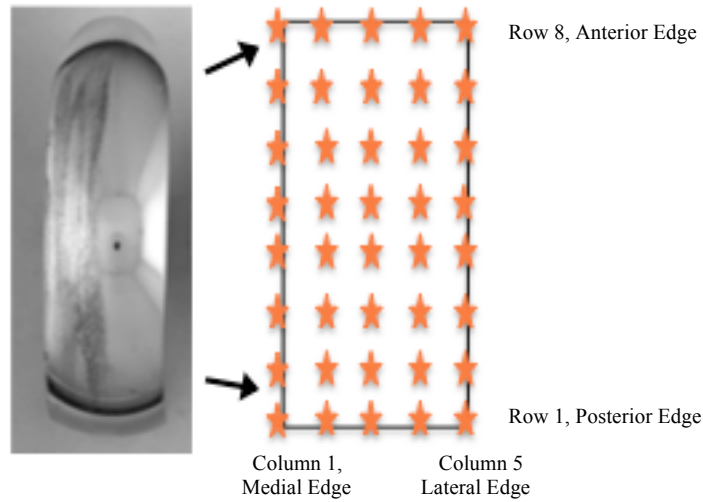


Figure 2.5: Distribution of 40 regions equally spaced, covering entire articular surface of femoral component and corresponding zones for analysis

A grid of 40 points was chosen based on the work of Alvarez et al, which determined that acquisition of data from at least 40 regions distributed across a bearing surface is necessary to adequately characterize surface roughness on retrieved knee replacements. [2] These 40 regions were then grouped into corresponding zones, eight rows spanning the articular surface from the posterior to anterior rim and five columns spanning the articular surface from the medial to lateral edge. In this manner, the tibial and femoral articular surfaces could be analyzed separately and then combined as a single bearing couple.

Articular surface damage on the femoral components was quantified in each of the 40 regions using a non-contact surface profilometer (WYKO NT2000, Veeco Corp., Tucson, Arizona) with a magnification of $\sim 25X$ (field of view $736 \times 480\mu\text{m}$, $\pm 0.1 \text{ nm}$ resolution). Each femoral component was positioned within an aluminum box such that the flat fixation surface of the posterior condyle was flush with the exterior face of the

box and then secured using SuperDent dental acrylic (MainStar America LLC, Miami, FL). Each femoral component was then mounted onto a customized jig, allowing for controlled positioning in the sagittal and frontal planes during analysis, as seen in Figure 2.6.



Figure 2.6: UKA femoral component mounted on customized jig and placed on stage of non-contact profilometer, demonstrating ability to control motion in frontal plane (left) and sagittal plane (right)

Surface roughness measures at each of the forty regions included R_{pm} , R_{vm} , R_v , R_a , R_p , R_t , R_z , and R_q . These parameters were chosen due to their relevance to previous studies of metal surfaces in joint replacement. [2, 28, 34, 36, 66, 72, 75, 77] These parameters are described in Table 2.3 and also in Figure 2.7. The roughness data presented for each component represents the average for all 40 measurements acquired across each articular surface.

Symbol	Parameter	Description
Ra	average roughness	Arithmetic average height calculated over the measured surface
Rp	maximum profile peak height	Distance between the highest point and the mean surface
Rpm	mean profile peak height	Average of 10 highest peak heights (Rp) on the surface
Rq	root mean square	Average between height deviations and the mean surface
Rt	maximum peak to valley height	Distance between the highest peak and lowest valley
Rv	maximum profile valley depth	Distance between the lowest point and the mean surface
Rvm	mean profile valley depth	Average of 10 lowest valley depths (Rv) on the surface
Rz	mean maximum profile	Average of 10 greatest peak-to-valley separations on the surface

Table 2.3: Description of collected surface roughness parameters

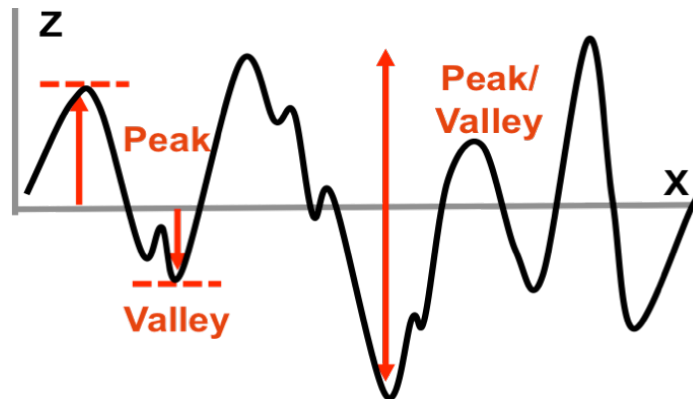


Figure 2.7: Simplified visual of peaks, valleys, and peak-to-valley separations on surface of metallic femoral component

Surface damage on the femoral components also was characterized using a reflected light optical stereomicroscope with lenses providing for magnification of 6x to 50x (model K400P, Motic Inc., Xiamen, China). Each of the 40 regions was photographed at 6x and 12x using the stereomicroscope, and corresponding digital images (300 x 300dpi) were compiled such that the entire articular surface could be

qualitatively analyzed. The incidence of eight characteristic metallic bearing damage modes (circular abrasion, linear abrasion, scratching, pitting, material transfer, tool damage, dulling, and fracture) were visually assessed according to previously published methods (Figure 2.2). [3]

The prominent surface damage mode present in each zone was identified by three experienced observers using the illustrative damage atlas, [3] with the mode resulting in consensus between the observers used as the defining damage mode for each given region. These prominent damage modes were determined for all 40 regions on each UKA to determine the frequency and coverage of specific damage modes. Frequency was defined as the percentage of UKA with the damage mode present in at least one of the 40 regions. Zone coverage was the average of the number of zones with each specific damage mode represented as a percentage of all 40 zones.

The methods used to characterize the femoral and tibial bearings assessed the entire articular surface rather than selecting areas with visibly extreme damage.

Results

Variations in surface roughness of the retrieved femoral components were evident based on gross microscopic assessments. These variations were accompanied by varying modes of damage and degrees of wear experienced by the coupled polyethylene. The average Ra and Rpm values for all nineteen UKA were 41.6 ± 48.6 (range 19.8-240.1) nm and 296.1 ± 212.0 (range 147.0-1102.6) nm, respectively.

A total of 15 components had associated duration of function recorded from the medical records and were used for evaluating changes in surface roughness relative to in

vivo duration. Despite a broad range of functional in situ time experienced by these UKA, the Ra and Rpm values did not change significantly following in vivo duration. When average roughness (Ra and Rpm) is plotted versus in situ, there was no significant correlation (linear regression $R^2 < 0.1$, $p = 0.558$), Figure 2.8 and 2.9).

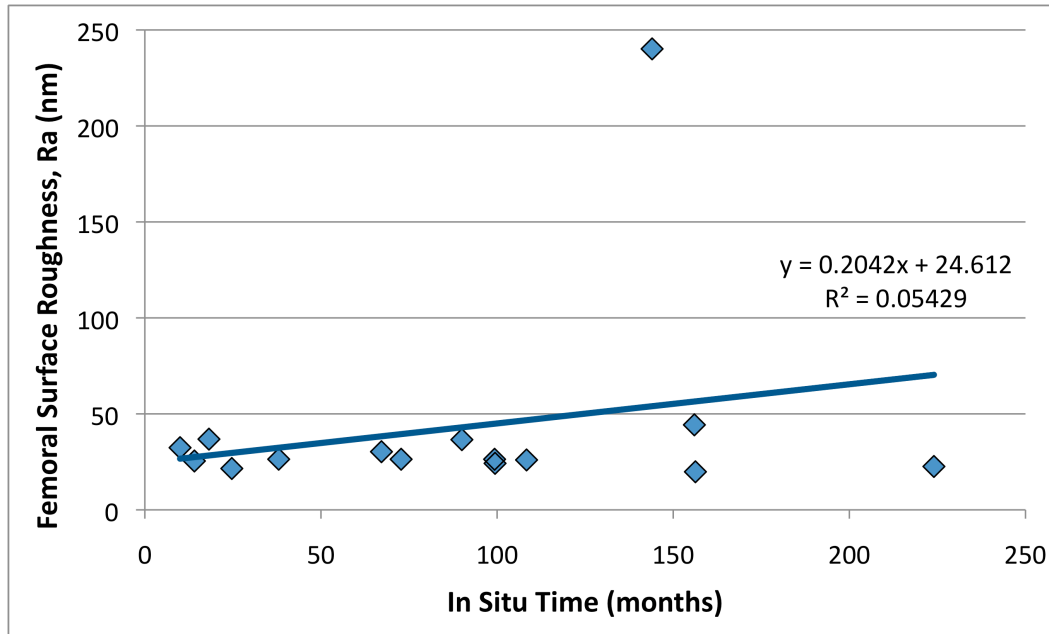


Figure 2.8: Average UKA femoral component surface roughness (Ra) versus in situ time.

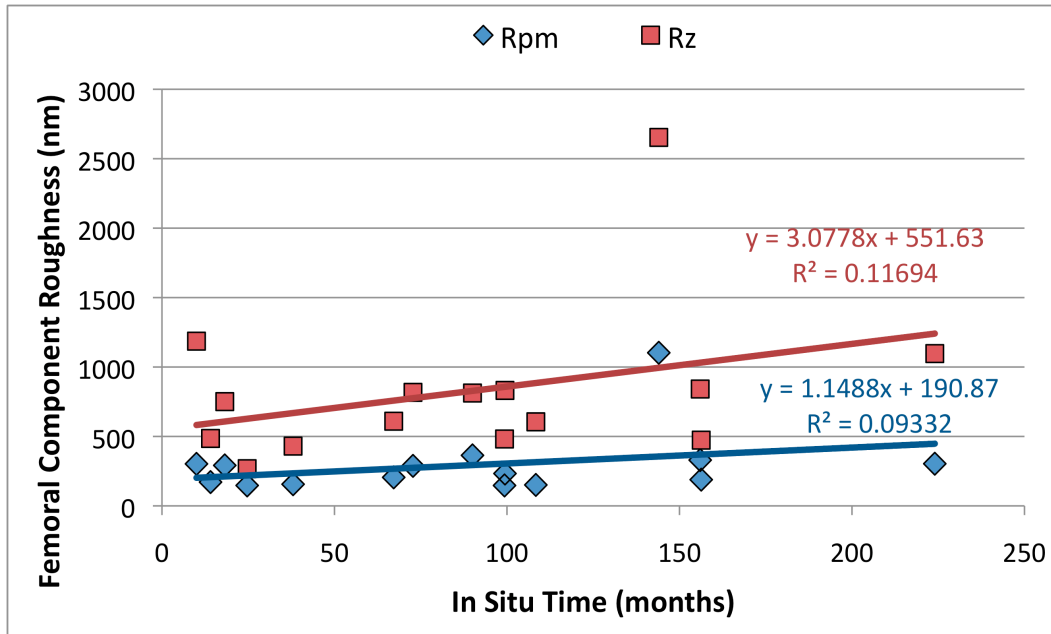


Figure 2.9: Average UKA femoral component profile peak height surface roughness (Rpm) and mean maximum profile (Rz) versus in situ time

Within the specimen collection, one UKA with notably high Ra and Rpm values was noted. This component functioned for an extended period of time (12 years) and had evidence of extra-articular abrasion associated with contact between the femoral bone and the periphery of the polyethylene insert (Figure 2.10).

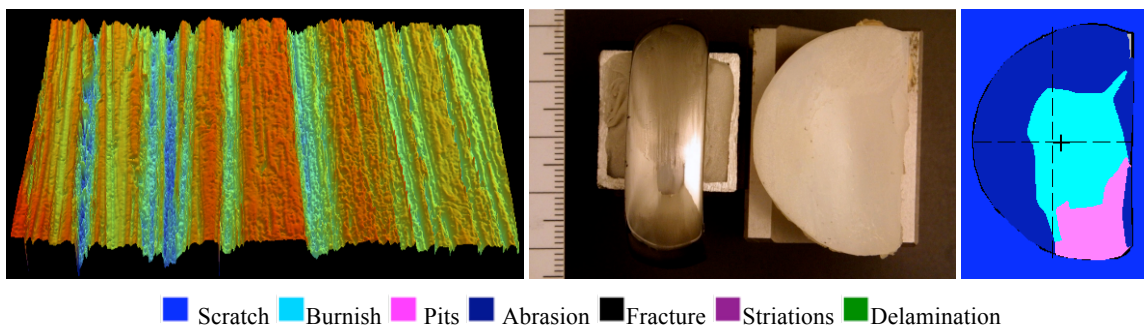


Figure 2.10: Representative 3D profilometry surface data of femoral component (left), gross photograph (19 pixels/mm) of femoral and tibial components in anatomical position (center), and polyethylene damage map (right) are shown for the outlying UKA with severe abrasive damage and associated high femoral surface roughness values

Damage area on the polyethylene inserts averaged 57.7 ± 24.0 (range 16.7-99.7) %, with scratching (13/19, 68%), abrasion (12/19, 63%), burnishing (10/19, 53%) and pitting (10/19, 53%) as the most common damage modes. Polyethylene damage area is reported as the surface area damaged as a percent of the total articular surface area. Despite a large variation in polyethylene damage modes, surface roughness values showed no statistical correlation to mode of polyethylene damage or polyethylene damage area, as seen in Figures 2.11 and 2.12.

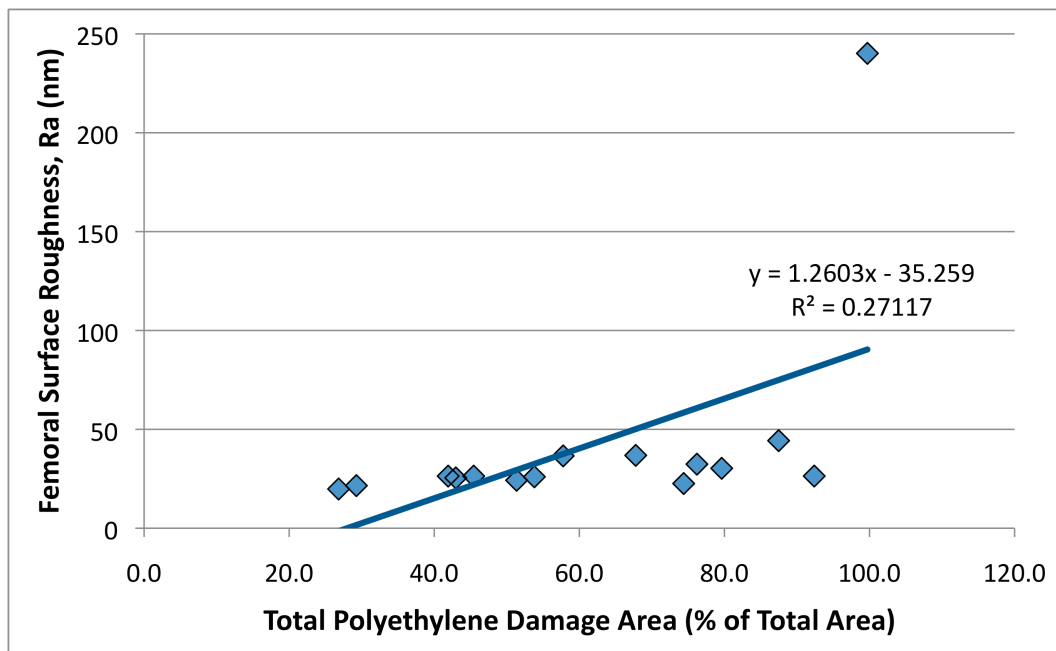


Figure 2.11: Average UKA femoral component surface roughness (Ra) versus total polyethylene damage area. Total polyethylene damage is reported as the surface area damaged as a percent of the total surface area

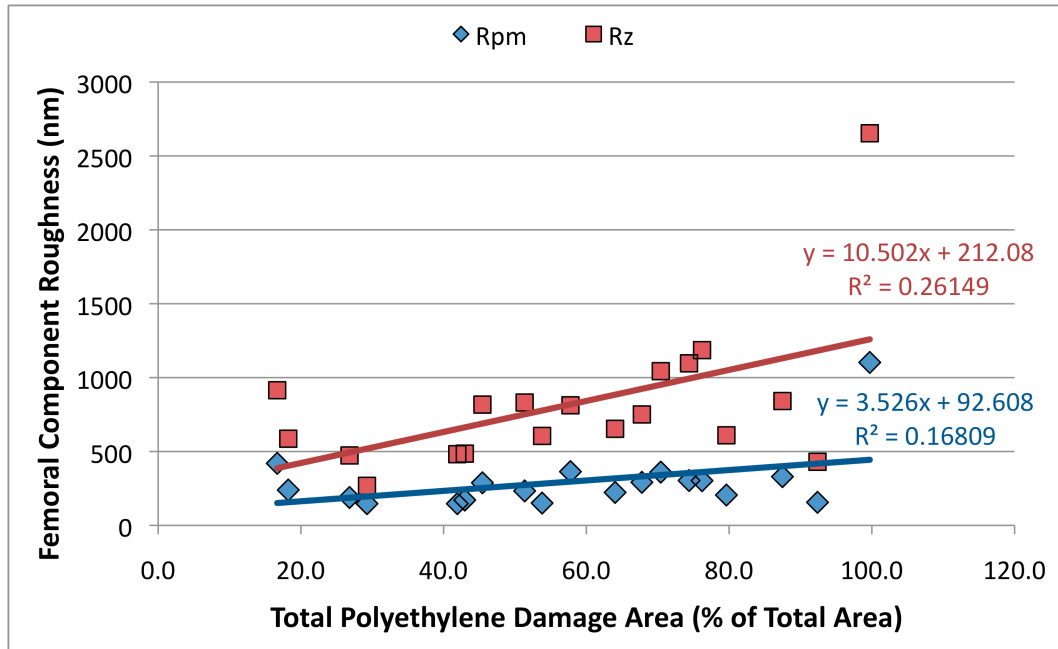


Figure 2.12: Average UKA femoral component profile peak height (Rpm) and mean maximum profile (Rz) surface roughness versus total polyethylene damage area. Total polyethylene damage is reported as the surface area damaged as a percent of the total surface area

The most commonly observed damage modes on the articular surfaces of the metal femoral components included scratching (18/19, 95%), abrasion (10/19, 53%), and pitting (6/19, 32%). Disregarding tool damage, or removal marks, and no damage, scratching was observed most frequently and was one of the most prominent modes evident in 24% of the zones. Even though scratching covered a large portion of the articular surface, its impact on the surface topography (Ra, Rpm, and Rz) was less than material transfer. In general, scratches and linear abrasion on the metal bearings were oriented in the direction of sliding motion (antero-posterior). Damage mode was a significant factor in the variance of roughness values (Kruskal-Wallis one-way ANOVA, $p < 0.05$).

Damage Mode	Zone Coverage			
	(%)	Ra (nm)	Rpm (nm)	Rz (nm)
Abrasion (10/19)	17 ± 14 (3-40)	30 ± 17 (13-115)	238 ± 202 (86-1209)	705 ± 664 (183-4064)
Scratching (18/19)	24 ± 19 (3-70)	33 ± 15 (13-100)	282 ± 409 (89-4700)	733 ± 619 (179-6753)
Pitting (6/19)	35 ± 40 (3-98)	27 ± 11 (11-61)	275 ± 132 (91-854)	1107 ± 392 (303-2309)
Material Transfer (2/19)	38 ± 35 (13-63)	293 ± 198 (30-789)	1110 ± 616 (205-2733)	2849 ± 1398 (584-5868)
Removal Marks (19/19)	15 ± 9 (3-35)	45 ± 49 (9-392)	426 ± 904 (67-7829)	1024 ± 1434 (149-11396)
No Damage (16/19)	51 ± 25 (8-95)	28 ± 13 (12-172)	215 ± 305 (70-5063)	605 ± 530 (125-7444)

Table 2.4: UKA femoral component visual damage modes, zone coverage and corresponding roughness values, displayed as mean ± standard deviation (range)

Using optical stereomicroscopy and the damage atlas to qualitatively assess the metallic femoral components, two were believed to exhibit material transfer. Components experiencing material transfer contributed to the highest Rpm and Rz values in comparison to the rest of the damage modes. Upon gross, visual assessment, neither component showed evidence of polyethylene wear-through, leading to contact between the tibial baseplate and femoral bearing surface.

Discussion

This study explored the relationship between femoral component surface roughness, polyethylene insert damage and in vivo duration through evaluation of metal-polymer bearing couples of UKA that were retrieved after an average of 88.1 months of in vivo function. Contrary to the first hypothesis, the magnitude of femoral component surface roughness did not increase with longer duration of function. Contrary to the second hypothesis, increased surface roughness did not correlate with greater areas of polyethylene damage when UKA with intact polyethylene inserts were considered. Based

on these findings from a small collection of UKA, assumptions of increasing surface roughness and high roughness values after long-term in vivo function are not supported, especially when the polyethylene tibial insert remains intact. In vitro simulations that report dramatic increases in surface roughness following testing may not be representative of physiologic conditions.

Controlled tribological studies have shown that polyethylene wear debris production is largely affected by the number of scratches, rate of their formation, and number of cycles they are in contact with the polyethylene surface. [34] Therefore, preventing, or reducing, the potential for damage caused by surgical tooling, third body abrasion, and formation of surface scratches on the metal surface could significantly decrease the amount of polyethylene wear by minimizing surface roughness. [28, 34, 35, 39, 72, 77, 78, 80] In the current study, the surface roughness values associated with in vivo function of these retrieved UKA were within values reported in other relevant studies (Table 2.5).

Femoral Component	Function	Ra (nm)	Rpm (nm)	Rp (nm)	Rz (nm)	Rq (nm)	Rt (nm)	Ref.
New	None	7-42	140-385		66-306	10-41		[3, 45, 54]
Tumble Roughened	None	77-175	510-1896		253±22			[45]
Tumble Roughened	In Vitro	170-189	1243-1499					[45]
Retrieved	None	30-400	200-3900	100-4200	931-2675	67.9-172	330-5860	[3, 17, 48, 54]
Retrieved	In Vitro	90-360		380-2120				[48]
Current Study	None	41.5 (20-240)	296.0 (147-1103)	434.9 (194-1241)	818.0 (268-2653)	57.7 (27-326)	1518 (455-3190)	

Table 2.5: Reported surface roughness values and current study median values with associated range

The surface roughness values resulting from in vivo function are notably lower than those of prostheses functioning in controlled, in vitro studies. In general, in vitro studies artificially roughen the femoral components by tumbling them in an abrasive media, such as alumina powder, resulting in scratches more severe in degree and of a random orientation. [72] Some studies also have reported that following artificial roughening, the scratches are shorter in length [78] and appear to be less dense and less uniform [77] than scratches visualized on retrieved femoral components. Some of the disparities in surface roughness experienced in vivo are caused by differences in time when roughening occurred, location of roughening, and composition of joint fluid. [80] Subsequent to increased roughness values, in vitro studies using artificially roughened femoral components also usually overestimate polyethylene wear volume and/or wear rates compared to in vitro studies using retrieved components and in vivo studies. [80]

Scratches observed on components following in vivo service are predominantly located in the anterior-posterior direction, such that they are parallel to the wear sliding direction; thus, studies utilizing tumbled, femoral components with more severe and randomly oriented scratches would be expected to report increased polyethylene wear. [72, 77] In vitro studies also will overestimate wear values because abrasive wear tests are generally performed such that the metal counterfaces begin with and maintain an extremely roughened surface throughout the entirety of the test. Conversely, in vivo roughened components may not experience roughening until a late stage of the functional duration, which will then result in a period of rapid polyethylene wear and subsequent revision. [80]

The UKA analyzed in this study showed no significant correlation between increase roughness values and prolonged implantation time. Hence, physiological function does not always increase the surface roughness of the femoral components (Figures 2.8 and 2.9). Excluding the extreme sample that underwent extra-articular abrasion, the remaining prostheses showed a very small range of average roughness (Ra) values, between 20 and 55mm. Similarly, several other retrieval studies also have reported findings demonstrating no correlation between in situ time and surface roughness values, specifically Ra-average roughness, [36, 45, 66, 77] Rp= maximum profile peak height, [66] Rpm- mean profile peak height, [66] Rz- mean maximum profile, [36, 85] and Rq- root means square. [36] Even though in vitro studies attempt to mimic physiological conditions, the values reported by these studies are likely not

representative of in vivo function, explaining why their values are much higher than those reported in the current study.

The retrieved prostheses of this study also demonstrated no correlation between femoral component surface roughness and damage area or mode of damage experienced by the polyethylene component. However, it was evident that one femoral component experienced severe abrasion damage, resulting in extreme surface roughness values upon analysis (Figure 2.10). Further detailed assessments of this one UKA are needed to determine possible factors contributing to this observation. It should be noted that the present study measured damage area of the polyethylene insert not wear volume, while the relationship determined by Dowson, et al explained volumetric wear of the polyethylene resulting from increased roughness of the femoral component. [35] Variations in damage area have been linked with knee kinematics during activities of daily living, which may mask possible relationships between femoral roughness and polyethylene damage area. [15, 50]

Visual assessments and quantification of damage applied to both the metallic and polyethylene components provided a linked evaluation of in vivo performance for both bearing materials in the UKA bearing couple. This study reported similar damage distributions as other retrieval studies, with scratching as the most common damage mode evident on nearly all-metal articular surfaces. The variation in surface roughness parameters showed a wide distribution for all reported damage modes. Excluding material transfer, the average surface roughness (Ra) for the metallic damage modes was within the manufacturing tolerance for surface finish of femoral components (typical

range: 20-59nm). Femoral components with material transfer showed the highest Ra, Rpm and Rz values with an average of 38% zone coverage. In addition to alignment and fixation, [52] these data support that maintaining femoral component roughness less than 50nm contributes to a polyethylene deformation rate of less than approximately 0.2mm/year.

There were some limitations to this study. Sample size was relatively small with substantial variations in prosthesis designs of both the femoral components and polyethylene tibial inserts, including geometry, size and manufacturing processes. There were also differences in the location of implantation, though the majority was implanted in the medial condyle, and likely discrepancies in surgical technique among surgeons. All types of polyethylene wear that could possibly occur in vivo were not necessarily represented on all samples, further limiting the sample size that could be correlated to each damage mode. Limited available patient data in 4 UKR with unknown duration of function, for example, also contributed to narrowing of the sample size available for correlation with surface roughness.

CHAPTER THREE

STUDY 2: MODE II WEAR

Introduction

Continuing the discussion of wear that occurs at bearing surfaces, mode II wear occurs when a primary bearing surface articulates against a nonbearing surface in a manner not intended by the designers. [14, 70] This phenomenon occurs in TKA when the prosthesis experiences complete wear through of the polyethylene insert, leading to contact between the articular surface of the femoral component and the underlying tibial baseplate. This metal-on-metal contact potentially leads to an increased surface roughness of the articular surface, resulting in further wear of the polyethylene and generation of tremendous amounts of wear debris. The wear is generally both polymeric and metallic in nature and typically results in osteolysis and/or aseptic loosening of the prosthesis ending in revision surgery.

Depending on the hardness and material properties of the surfaces, adhesive wear is generally one of the main mechanisms following mode II wear that leads to material transfer onto the articulating surface. Adhesion is the formation and segregation of bonds between the two counter bearing surfaces, which is a function of relative velocity, load and contact area. [43] If the atomic forces between the two surfaces in contact are stronger than the cohesive molecular bonds of the softer material, the adhesive inter-material bonding will destroy the cohesive bonds of the weaker material with relative motion. [41, 43]

Typical materials used to fabricate TKA femoral components consist of metal alloys, mainly Co28Cr6Mo and Ti6Al4V. Recently, metals with a ceramic surface, like oxidized zirconium alloy, also have been used to achieve ceramic surface properties with a decrease in the risk of brittle fracture due to the underlying tough metal materials. A table of material properties of typical materials used to fabricate components of TKA is below (Table 3.1).

Metallic Material	Ultimate Tensile Strength (MPa)	Yield Strength (MPa)	Modulus of Elasticity (GPa)	Rockwell Hardness A (HRA 50)	Microhardness (HM 0.5)
Ti6Al4V	860-930	758-869	110	15-20	1500-1600
Co28Cr6Mo	655-1172	450-827	210	18-25	1400-1600
Zr-2.5Nb	450-600	310-434	97	10-15	1300-1500
Ceramic Material	Fracture Strength (MPa)	Fracture Toughness (MPa*m^{1/2})	Modulus of Elasticity (GPa)	Rockwell Hardness A (HRA 50)	Microhardness (HM 0.5)
Oxidized Zr-2.5Nb	220-234	2.00-2.06	190-199	35-40	1300-1500
Polymeric Material	Ultimate Tensile Strength (MPa)	Yield Strength (MPa)	Modulus of Elasticity (GPa)	Impact Strength (kJ/m²)	Fracture Toughness (MPa√m)
UHMWPE (Compression Molded)	26.2-35.8	17.6-24.9	.711-1.087	179	4.7
UHMWPE (Ram Extruded)	24-52.0	18-27.5	.710-.750	134	3.6

Table 3.1: Material properties of typical materials used to fabricate components of TKA and UKA[5–9, 12]

Metals are favorable materials for bearing surfaces of TKA due to their high strength, which prevents fracture, and their high toughness and modulus of elasticity, which prevents fatigue. The material and mechanical properties of these metals depends

heavily on the manufacturing method chosen to fabricate the components. Often these alloys are either cast or wrought; however, they also can undergo processes such as annealing or cold working to improve and optimize their mechanical performance. Titanium is often used as a biomaterial in TKA due to its exceptional biocompatibility and elastic modulus that is similar to bone; however, its low scratch resistance makes it less appealing for use as a femoral component. [42] Cobalt chromium alloys are often used in knee joints because of their high hardness, but studies have shown retrieved prostheses with scratch depths between 1 to 10 μ m, resulting in an increased surface roughness and potentially greater debris generation when articulating against polyethylene. [42] Metals used in vivo present with a thin passive oxide layer, typically less than 10nm thick, that acts to increase biocompatibility and protect the metal against corrosion and wear. [89] Depending on the lubrication layer between bearing surfaces, this passive layer cannot always withstand the shear forces generated by friction during joint articulation. [89] Removing the passive film exposes the less wettable surface of the bulk metal with a higher coefficient of friction, resulting in a greater potential for adhesive wear. [89]

It is generally believed that ceramics offer an increased hardness and scratch resistance with decreased surface roughness compared to metallic bearing surfaces. [65] Oxinium (Smith & Nephew, Memphis, TN) is a new material consisting of a zirconium alloy (Zr-2.5Nb) core that has been oxidized, producing a Zirconia (ZrO₂) ceramic surface. This material is produced by high temperature oxidation, which creates a gradient of diffused oxygen in the substrate, allowing the material to possess a gradual

transition of chemical, mechanical and physical properties (Figure 3.1). [32] Due to the mechanically stable ceramic surface that is 4-5 μm thick, this material is known to have high resistance to abrasion, adhesion and delamination. [32, 42, 43, 53, 78, 89] Several studies have shown this damage resistant surface results in rates of polyethylene wear that are more than six-fold less than articulation against CoCrMo femoral components. [32, 44, 79] Although the material is known to have high hardness and toughness with decreased surface roughness and excellent bonding between the ceramic and metallic layers, the underlying bulk material has the least favorable properties of all metals used for bearing surfaces in knees. [42, 89]

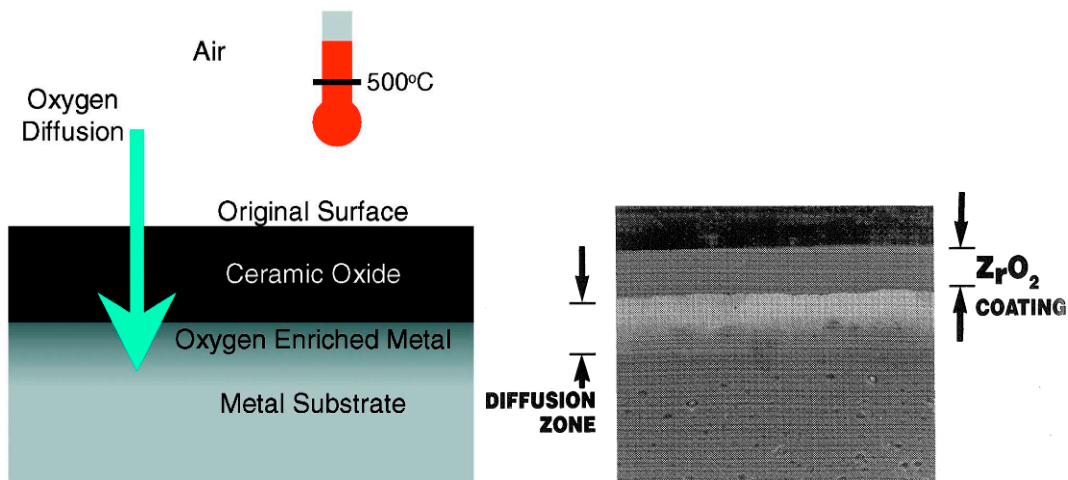


Figure 3.1: Simplified depiction (left) [79] and photomicrograph (right) [31] of oxidized zirconium alloy

Ultra-high molecular weight polyethylene (UHMWPE) is generally used to manufacture tibial inserts; however, there are various manufacturing processes, sterilization processes, and additives that change the material properties depending on the manufacturer. [21] Medical-grade polyethylene is a semicrystalline polymer that has

ordered regions embedded in an amorphous phase, with increasing crystallinity leading to increased modulus of elasticity, increased yield strength and fatigue strength, and greater resistance to creep deformation. [21] Both resistance to creep and increased fatigue strength help the material to resist damage modes typical of knee replacement prostheses under cyclic loading. [21] However, studies also have reported that molecular mass is related to wear resistance. [21] Improving and optimizing these material properties is critical to developing a tibial insert that is more resistant to delamination and fracture in order to prevent the catastrophic failures of prostheses due to complete polyethylene wear through, as seen in the present study.

The purpose of the present study is to characterize the damage of retrieved knee replacement bearing couples that have experienced complete polyethylene wear-through, while considering the material properties of the metal alloys. This study aims to compare material properties of common alloys used to fabricate femoral components and tibial baseplates, including cobalt-chrome alloy, titanium alloy, and oxidized zirconium alloy. It is hypothesized that material properties of the alloys will correspond with surface roughness, material transfer, and surface deformation or loss of material that occurs in the presence of polyethylene wear through and mode II wear.

Materials and Methods

Four TKA and three UKA were retrieved during revision arthroplasty at five institutions located in the United States (Good Samaritan Medical Center, West Palm Beach, Florida; Palm Beach Gardens Medical Center, Palm Beach Gardens, Florida; Patewood Memorial Hospital, Greenville, South Carolina; AnMed Health Medical

Center, Anderson, South Carolina) and Germany (University Hospital Mannheim, University of Heidelberg, Mannheim, Germany) over an eighteen-year period (1994-2012). These UKA and TKA were archived in two established, institutional review board approved Implant Retrieval Programs. [49] Using a database search, prostheses with complete wear through of polyethylene tibial inserts were identified. The prostheses were included if all major components of the replacement prostheses, including the femoral component, tibial base-plate and tibial polyethylene insert were available for analysis.

Surgical technique included implantation of one UKA in the lateral compartment and two UKA in the medial compartment. All UKA had non-conforming tibio-femoral articulations with fixed-bearing polyethylene inserts and included designs fabricated by 2 different manufacturers (Table 3.2). Cement fixation was used for all 3 of the UKA femoral components and tibial components. All TKA also were round-on-flat tibio-femoral articulations and had various fixation methods on their femoral and tibial components (Table 3.2). All TKA had fixed bearing polyethylene inserts and included 3 designs by different manufacturers (Table 3.2). At this time, the polyethylene materials (ram-extruded or compression molded) and sterilization methods (gamma radiation or ethylene oxide) could not be determined for all prosthesis designs since the original packaging labels were not available.

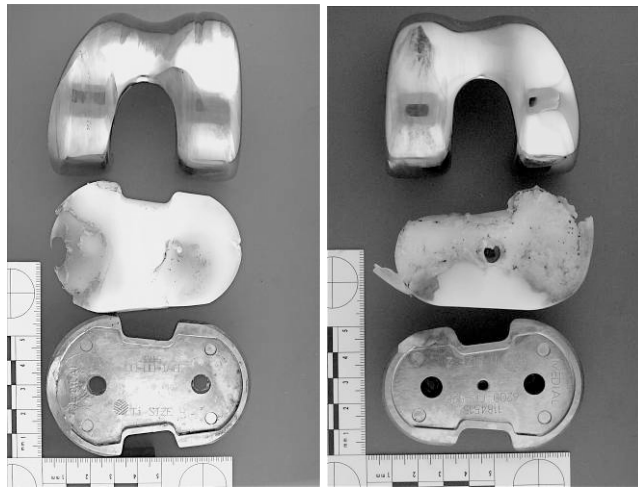
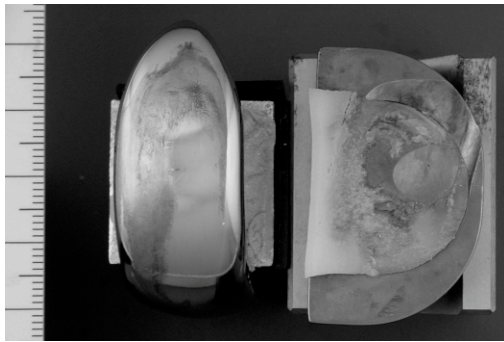
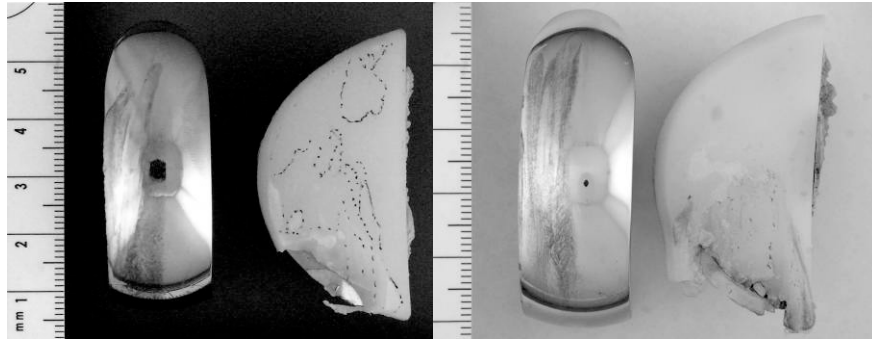
Prosthesis #	Manufacturer	Conformity**	Tibial Base Plate	Bearing	Fixation*	Implantation Site
UK2081_94R	Johnson & Johnson	Unknown	Metal-backed	Fixed	F & T Cemented	Lateral
UK2024_04R	Link	ROF	Metal-backed	Fixed	F & T Cemented	Medial
UK2026_04R	Link	ROF	Metal-backed	Fixed	F & T Cemented	Medial
K1283_04L	InterMedics	ROF	Metal-backed	Fixed	F & T Cementless	N/A
K2044_11R	InterMedics	ROF	Metal-backed	Fixed	F & T Cementless	N/A
K247_12L	Richards	ROF	Metal-backed	Fixed	F & T Cemented	N/A
K271_12L	Smith & Nephew	ROF	Metal-backed	Fixed	T Cemented, F Cementless	N/A

*Fixation method was determined for both femoral (F) and tibial (T) components

**Conformity was defined to be round-on-flat (ROF) or unknown.

Table 3.2: Available data on retrieved UKA and TKA prostheses

Figure 3.2 demonstrates all prostheses analyzed in the current study, including their material composition. Four material pairs were identified from these prostheses with mode II wear and metal-on-metal contact. Cobalt-chromium-molybdenum (CoCrMo) alloy femoral components and CoCrMo tibial baseplates were used in 2 UKA. CoCrMo femoral components and titanium-aluminum-vanadium (TiAlV) alloy tibial baseplates were used in 1 UKA and 2 TKA. A TiAlV femoral component and TiAlV baseplate were used 1 TKA. Finally, an Oxinium (Smith & Nephew, Memphis, TN) femoral component and TiAlV baseplate was used in 1 TKA. Each of the tibial inserts for the TKA and UKA were composed of UHMWPE. This information is simplified in Table 3.3.



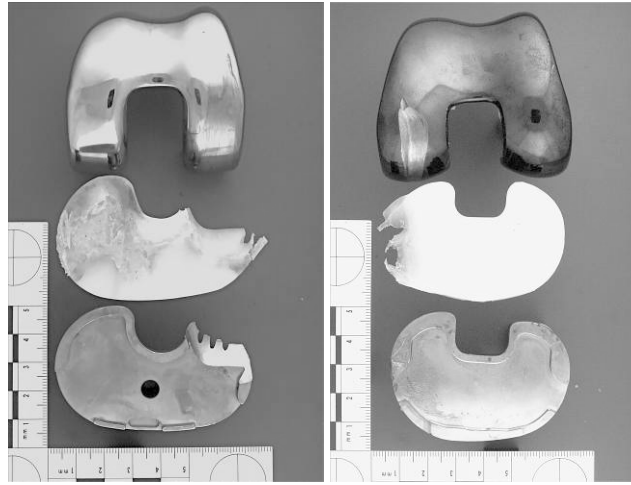


Figure 3.2: UKA and TKA prostheses analyzed in the current study, including (A) Endosled Waldemar Link UKA from Germany, (B) Johnson & Johnson UKA, (C1, C2) InterMedics Natural Knee, (D) Richards TKA and (E) Smith & Nephew Genesis II

Prosthesis #	Tibial Insert	Femoral Component	Tibial Baseplate
UK2081_94R	UHMWPE	CoCrMo	TiAlV
UK2024_04R	UHMWPE	CoCrMo	CoCrMo
UK2026_04R	UHMWPE	CoCrMo	CoCrMo
K1283_04L	UHMWPE	TiAlV	TiAlV
K2044_11R	UHMWPE	CoCrMo	TiAlV
K247_12L	UHMWPE	Oxinium	TiAlV
K271_12L	UHMWPE	CoCrMo	TiAlV

Table 3.3: Material composition of UKA and TKA prostheses components

Patient demographics were obtained from available medical records and are summarized in Table 3.4. Included in this study were 5 females with a mean age of 66.5 (SD 9.5, range 55.0-78.2) years at index surgery and mean age of 73.6 (SD 7.7, range 64.0-84.9) years at the time of retrieval. All three of the UKA and one of the TKA were implanted in the right knee, while the remaining three TKA were implanted in the left. Average duration of in vivo function for these prostheses was 118.1 (SD 63.7, range 67.7-228.0) months.

Prosthesis #	Sex	Age at Index	Age at Retrieval	Time in situ (mos.)	Weight (kg)	Height (cm)	Revision Reason
UK2081_94R	F	55.0	64.0	108.0			PE wear, metallosis
UK2024_04R	F	67.7	76.5	105.6	92	151	aseptic loosening
UK2026_04R	F	65.0	70.6	67.7	82	162	aseptic loosening
K1283_04L			72.0				metallosis
K2044_11R							
K247_12L	F			81.0			aseptic loosening
K271_12L	F	78.2	84.9	228.0	82	173	PE wear, loosening
Average		66.5	73.6	118.1	85.3	162	
SD		9.5	7.7	63.7	5.8	11	

Table 3.4: Available clinical data for patient population

Following protocols established at both retrieval labs, all retrieved components were handled similarly: fixation in formalin, cleaning using a mild detergent, sonication, rinsing in clean water and ethanol, and air drying. Similar to Study 1, a component-based coordinate system was established for the bearing surfaces of the femoral components by using the fixation pegs and flat fixation surface for the posterior of the condyles (Figure 2.4). Reference features also included the posterior rim of both the UKA and TKA and either the anterior rim of the UKA or intercondylar notch of the TKA. The overall width of the and length of the articular surface of each individual femoral component was measured using a flexible ruler, subtracting 10% of the total length of the UKA, 5% of the total length on the TKA and 5% of the total width on both UKA and TKA to accommodate small shape deviations, since the bearing surface was not an exact rectangle.

Using the protocol defined in Study 1, the dimensions of the retrieved components were used to define a uniform 3-dimensional grid of 40 regions equally spaced across the entire articular surface of each femoral component (Figure 3.3). The 40-point grid, distributed in eight rows and five columns, was distributed across both condyles of the TKA and the single articular surface of the UKA, as they all share very similar geometry.

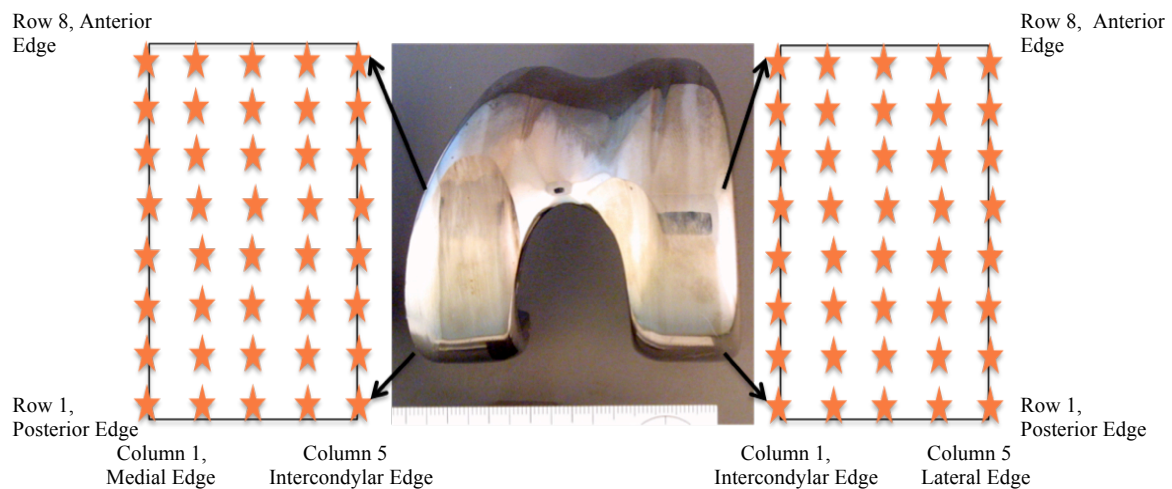


Figure 3.3: Distribution of 40 regions equally spaced across each condyle of TKA femoral component and corresponding zones for analysis

Femoral component damage of the articular surface was quantified in each of the regions of the 40-point grid using a non-contact surface profilometer. The three UKA were analyzed using the WYKO NT2000 (Veeco Corp., Tucson, AZ) with a magnification of ~25X (field of view 736 x 480 μ m, \pm 0.1 nm resolution), while the four TKA were analyzed with the NPFlex (Bruker Corp., Tucson, AZ) with a magnification of ~20x (10x lens and 2x multiplier, field of view 0.317 mm by 0.238mm, \pm 2-3 nm resolution). As in Study 1, each of the UKA and TKA were positioned and fixed within

an aluminum box, such that the flat fixation surface of the posterior condyle was flush with the exterior face of the box. Each of the femoral components was then mounted onto a customized jig, allowing for controlled positioning in the sagittal and frontal planes during analysis, as seen in Figure 3.4. Surface roughness measurements at each of the forty regions included the same parameters retrieved in Study 1, which are described in Table 2.3 and Figure 2.7. Again, these parameters were chosen due to their relevance to previous studies of metal surfaces in joint replacement. [3, 28, 34, 36, 66, 72, 75, 77]

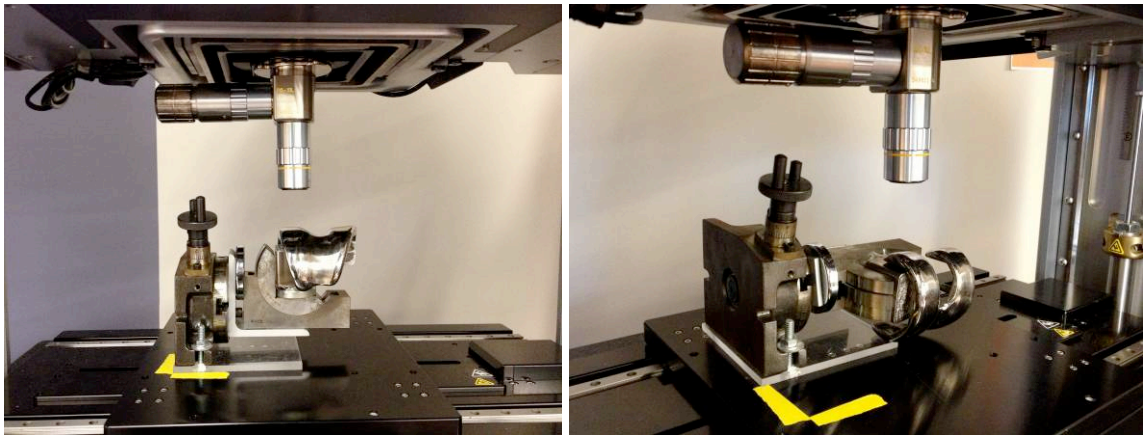


Figure 3.4: TKA femoral component mounted in aluminum block on customized jig and placed on stage of non-contact profilometer, demonstrating ability to control motion in frontal plane (left) and sagittal plane (right)

Surface damage on the femoral component also was characterized using a reflected light optical stereomicroscope with lenses allowing for magnification of 6x to 50x (model K400P, Motic Inc., Xiamen, China). Similar to Study 1, each of the 40 regions was photographed at 12x using the stereomicroscope and corresponding digital images (300 x 300 dpi) were compiled such that the entire articular surface could be qualitatively assessed. The prostheses were visually analyzed according to previously

published methods [3] for macroscopic dimensional changes in the articular surface, in addition to the incidence of characteristic metallic damage modes (Figure 2.2). [3]

The prominent surface damage mode present in each zone was identified by an experienced observer using the illustrative damage atlas, [3] with the defining damage mode described as covering the most surface area of each given region. These prominent damage modes were determined for all 40 regions on each UKA to determine the frequency and coverage of specific damage modes. Frequency was defined as the percentage of UKA with the damage mode present in at least one of the 40 regions. Zone coverage was the average of the number of zones with each specific damage mode represented as a percentage of all 40 zones.

In order to further investigate the damage on the femoral component articular surface, scanning electron microscopy (SEM S-3400N) was utilized at magnifications between 50x and 500x. The SEM also was equipped with Oxford INCA electron dispersive spectroscope (EDS) (Oxford Instruments, Abingdon, Oxfordshire) and a four-quadrant solid-state backscatter detector (BSECOMP). EDS was used to confirm the presence of material transfer and to determine material compositions of the transferred material on both the articular surface of the femoral component, as well as on visually damaged areas of a specific tibial baseplates. For the Oxinium component, both the femoral component articular surface and tibial baseplate were analyzed, since the TiAlV alloy of the baseplate and ZrNb alloy of the underlying surface of the femoral component can be of similar hardness. For SEM and EDS analysis, visually, macroscopic damage was found on each of the articular surfaces and chosen as the area of interest.

Surface damage on the polyethylene inserts were characterized using gross, macroscopic assessment and a previously published polyethylene damage mode atlas. [47] The inserts were qualitatively assessed for the incidence of ten different characteristic damage modes identified in Figure 2.1.

Results

All of the polyethylene tibial inserts experienced a variety of damage modes, most of which were easily visualized macroscopically. Most noticeably, each TKA and UKA tibial insert experienced both fracture and delamination. In addition, all of the TKA tibial inserts were found to have embedded debris, while each of the UKA inserts experienced abrasion.

Overall, the surface roughness values collected for both TKA and UKA that experienced complete polyethylene wear through were much higher than those measured in previous studies for components that underwent typical in vivo wear (Table 2.5). The average roughness (Ra) and maximum profile peak height (Rpm) for all of the articular surfaces measured in the current study averaged 142.8 ± 227.0 nm and 1045.7 ± 1222.9 nm, respectively. The TKA condyles of the current study demonstrated higher average roughness values (171.1 ± 257.5 nm) compared to their UKA counterparts (67.6 ± 67.4 nm). In addition, compared to the non-wear-through TKA condyles, those that had contacted the underlying metal tibial baseplate showed dramatically increased values of Ra (246.1 ± 237.3 nm versus 104.9 ± 257.1 nm) and Rpm (1830.0 ± 1519.0 nm versus 733.9 ± 917.9 nm). This is demonstrated further in a roughness plot for each of the 40 regions across the medial and lateral condyles of one specimen (Figure 3.5). The

roughness data presented for each articular surface represents the average for all 40 measurements acquired across each articular surface.

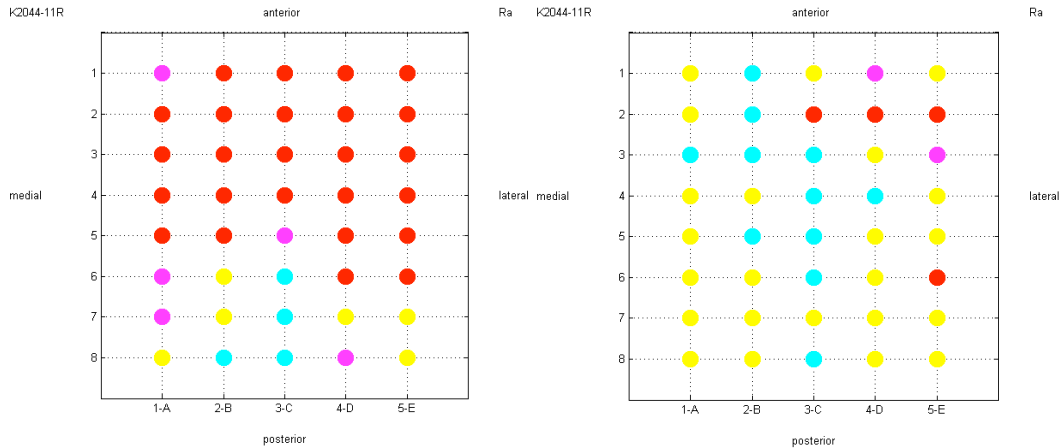


Figure 3.5: Roughness (Ra) plot of both TKA condyles where the lateral (left) experienced polyethylene wear-through and the medial (right) condyle did not. Red indicates a Ra value greater than 120 nm, pink indicates values between 81 and 120nm, yellow indicates values between 51 and 80nm, and cyan indicates values between 21 and 50nm

In order to understand how material properties may have influenced surface topography, the roughness parameters of each combination of materials of potential metal-on-metal bearing couples was compared. The results are presented in Table 3.5 below.

Bearing Couple Materials	Ra (nm)	Rpm (nm)	Rz (nm)
CoCrMo--CoCrMo	50 ± 39 (15-217)	386 ± 408 (90-2793)	981 ± 752 (177-4075)
CoCrMo--TiAlIV	138 ± 138 (22-924)	1216 ± 1200 (124-10838)	2461 ± 2124 (378-14469)
TiAlIV--TiAlIV	161 ± 141 (30-617)	953 ± 690 (208-3945)	2592 ± 1648 (255-8153)
Oxinium--TiAlIV	246 ± 492 (30-2676)	1398 ± 1982 (214-9441)	3392 ± 4985 (587-24085)

Table 3.5: Roughness values for varying potential metal-on-metal bearing couples of TKA and UKA

Surface roughness quantification of the Oxinium femoral component was unable to be completed in rows 2-5 due to the gross removal of the articular surface. This dimensional change in the surface was considered a rare catastrophic failure, such that taking the surface roughness of the underlying material would be irrelevant to our study. Thus, surface roughness values were only acquired for the surrounding articular surfaces, rather than the zones with deep removal.

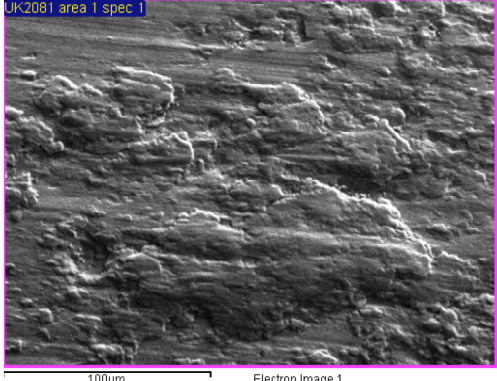
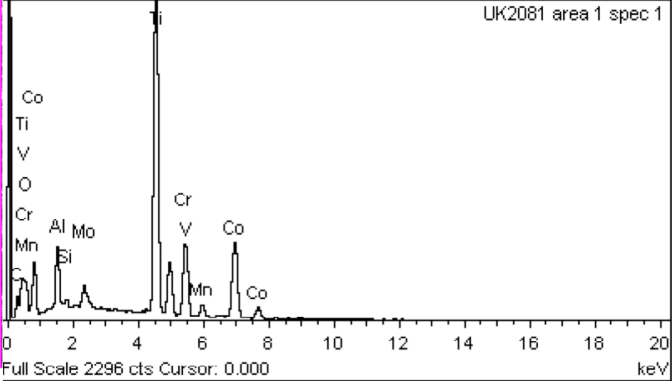

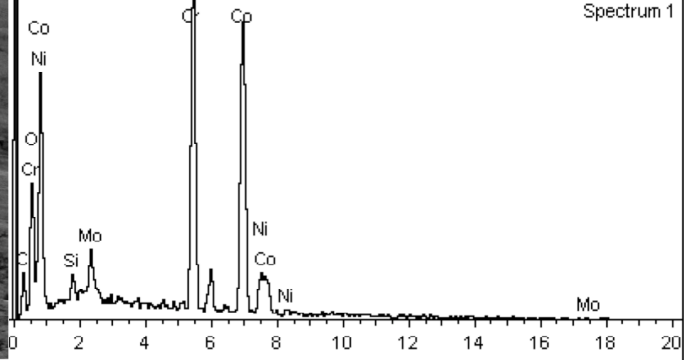
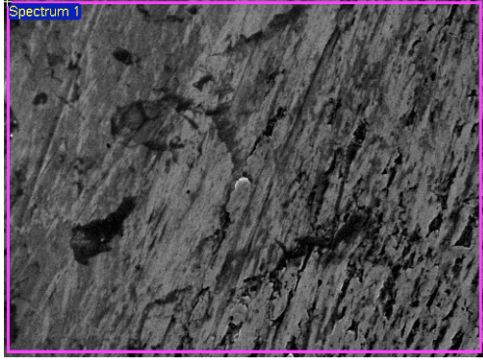
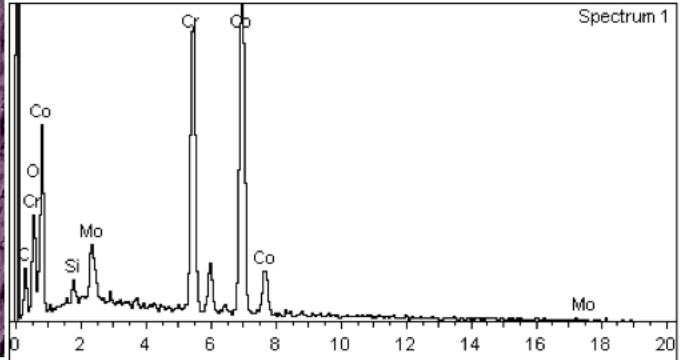


Figure 3.6: Gross image (left) and stereomicroscope image at 6x magnification (right) of gross removal of articular surface on Oxinium TKA femoral component

SEM analysis confirmed the presence of severe damage on the articular surface of bearing couples of the same material, including the CoCrMo alloy on CoCrMo alloy and

TiAlV alloy on TiAlV alloy, as well as couples composed of different materials. EDS analysis was then utilized to verify the presence of material transfer of the softer material onto the harder material of the bearing couples of different metallic composition. The results of this analysis are presented in Figure 3.7, demonstrating the area of interest on the articular surface, as well as the elemental composition for each area.

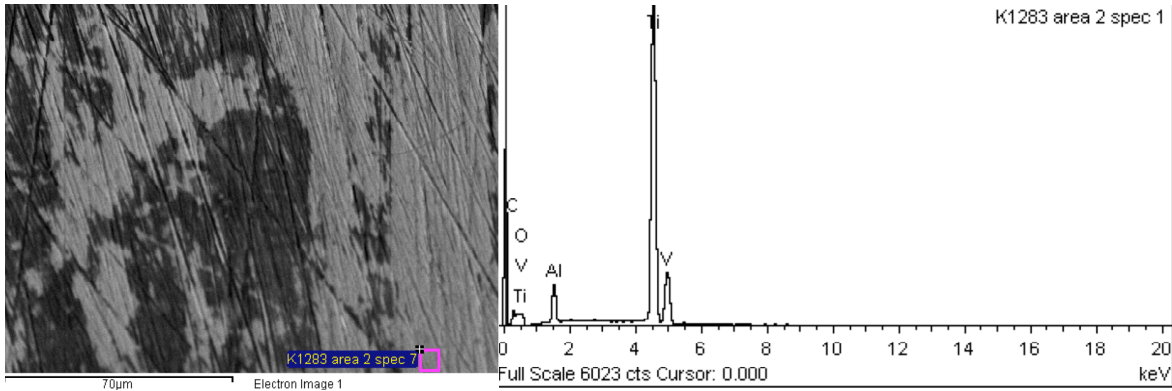
Femoral Component Analysis

Prosthesis #	Femoral Component Material	Tibial Baseplate Material
UK2081_94R	CoCrMo	TiAlV
		
UK2024_04R	CoCrMo	CoCrMo
		
UK2026_04R	CoCrMo	CoCrMo
		

K1283_04L

TiAlV

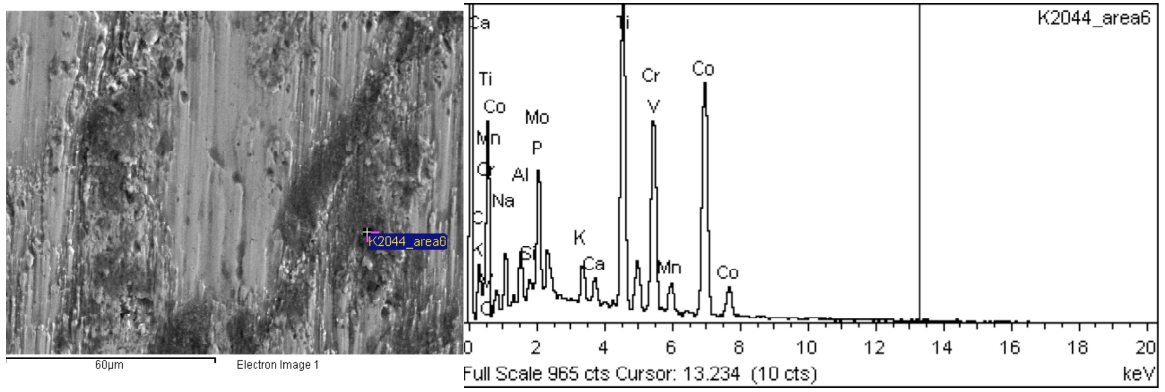
TiAlV



K2044_11R

CoCrMo

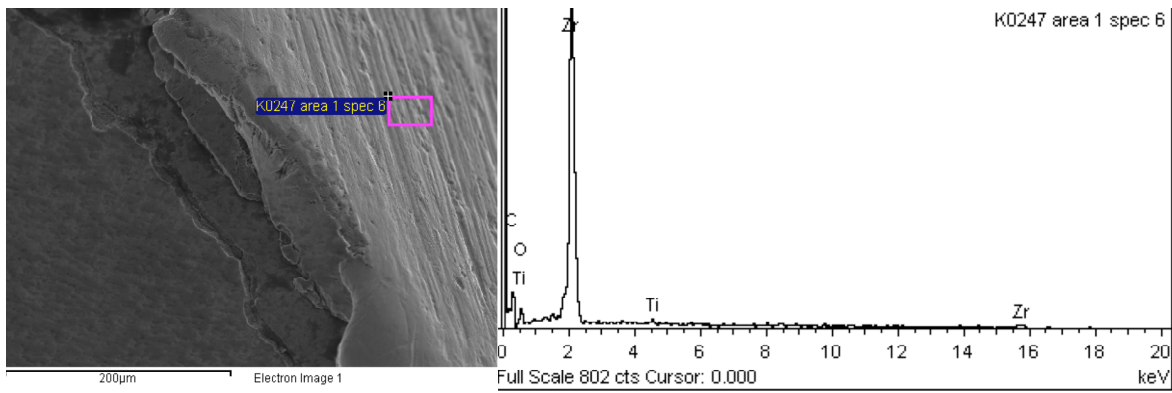
TiAlV

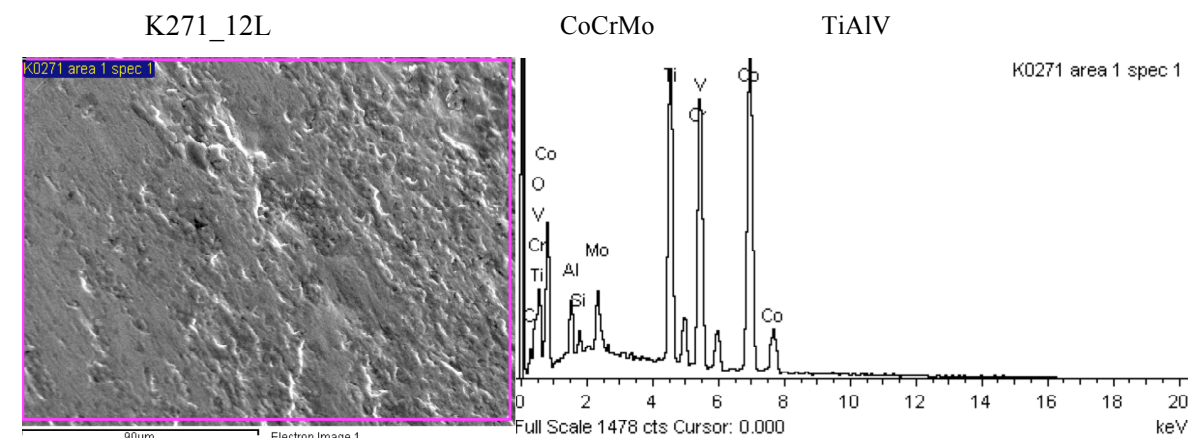


K0247_12L

Oxinium

TiAlV





Tibial Baseplate Analysis

Prosthesis #	Femoral Component Material	Tibial Baseplate Material
K247_12L	Oxinium	TiAlV

Figure 3.7: Bearing couple material, SEM images (50x-500x) of the area of interest and EDS elemental composition of the corresponding areas for each TKA and UKA of the present study

Metallic damage modes visualized on TKA and UKA with complete polyethylene wear-through were similar to those visualized on the non-wear-through components of Study 1; however, components with wear through experienced greater roughening with a greater frequency of material transfer and dimensional changes. Gross dimensional changes were seen on 5/11 components, covering an average of $28\% \pm 18\%$ of zones on

each surface. Excluding those that experienced macroscopic removal of material, a variety of damage modes were visualized on each component, as summarized in Table 3.6. Scratching was the most common mode of damage (11/11, 100%), followed by abrasion (9/11, 81%) and material transfer (6/11, 55%). Dulling and material transfer were the most prominent damage mode, covering an average of $51\% \pm 9\%$ and $50\% \pm 18\%$, respectively, of the zones on components that experienced these modes.

Damage Mode	Zone Coverage			
	(%)	Ra (nm)	Rpm (nm)	Rz (nm)
Abrasion (9/11)	13 ± 19 (3-63)	54 ± 22 (24-122)	504 ± 195 (141-968)	1073 ± 617 (378-2669)
Dulling (2/11)	51 ± 9 (45-58)	123 ± 78 (34-452)	734 ± 252 (310-1542)	2157 ± 1026 (530-5083)
Material Transfer (6/11)	50 ± 18 (28-75)	190 ± 152 (19-924)	1588 ± 1368 (131-10838)	3297 ± 2262 (235-14469)
Pitting (2/11)	4 ± 2 (3-5)	50 ± 24 (26-74)	421 ± 250 (152-645)	674 ± 261 (417-939)
Scratching (11/11)	16 ± 14 (3-40)	50 ± 20 (22-148)	535 ± 443 (124-3731)	1195 ± 1469 (355-12550)
Dimensional Changes (5/11)	28 ± 18 (13-50)	419 ± 514 (47-2676)	2127 ± 1916 (373-9441)	5058 ± 4020 (649-16565)
Removal Marks (5/11)	8 ± 5 (3-15)	198 ± 213 (18-696)	1670 ± 2050 (167-7162)	4621 ± 6989 (312-24085)
No Damage (5/11)	35 ± 20 (8-55)	39 ± 15 (15-73)	429 ± 464 (105-2793)	1000 ± 754 (177-4188)

Table 3.6: Femoral component visual damage modes, zone coverage and corresponding roughness values, displayed as mean \pm standard deviation (range) of each of the 8 condyles of TKA and 3 UKA characterized

Discussion

Complete wear through of polyethylene inserts leading to catastrophic failure of TKA is not a new phenomenon. [19] Excluding patient attributes, there are many factors that contribute to such extreme wear, including alignment during implantation, conformity of the articular surfaces, manufacturing and sterilization processing of the polyethylene, shelf age of the polyethylene at implantation, thickness of the insert,

surface roughness of the femoral counter bearing surface, and several other considerations. While improvements have been made in each of the aforementioned areas, wear-through leading to prosthesis failure continues to remain of clinical relevance, as demonstrated by the present study. When wear-through occurs, the typical damage on the metallic femoral and tibial components, due to their articulation, causes the revision surgery to be more complicated. [19] This type of damage requires replacement of all TKA components rather than simply replacing the polyethylene insert, indicating the need for earlier recognition of polyethylene wear. [19]

The three femoral UKA components and four femoral TKA components were cases of extreme wear caused by metal-on-metal contact following complete polyethylene wear-through. They are not representative of typical in vivo roughening that occurs due to femoral contact against a polyethylene bearing. They demonstrated heightened surface roughness values for all of the parameters measured. The contact between the cobalt-chrome alloy, titanium alloy, or Oxinium femoral component and the titanium alloy or cobalt-chrome alloy tibial base-plate results in a distinct region of either material transfer onto the bearing surface or catastrophic removal of material (Figure 3.7). These damage modes cause pile up onto the surface that is evident in Rpm values and removal that is shown in Rz values.

These particular components represent the roughening that accumulates with the cascade of failures associated with complete wear through. The average values of roughness measured for these particular prostheses (Table 3.6) is expected to be higher than values reported by manufacturers for new prostheses, which is between 20 and

50nm, due to their average in vivo duration of 118 months. However, these prostheses exhibited roughness values much higher, in some cases, than values measured in other studies, including those in Study 1 and Table 2.5. This demonstrates the immense destruction that occurs on the articular surface in the presence of polyethylene wear through. When contact between the femoral component and tibial baseplate occurs following wear through of the insert, this not only causes a roughening of the articular surface but it also causes further increases in polyethylene wear. This initiates a worsening cycle of polyethylene wear and articular surface damage that both lead to the production of tremendous amounts of wear debris, leading to osteolysis and loosening of the prosthesis requiring revision.

For TKA, it is not only the condyle that experienced polyethylene wear through that is of concern. The present study demonstrated that the condyle experiencing wear through had much higher values of roughness than non-wear through condyles; however, the values reported for non-wear through condyles (Ra of 104.9 ± 257.1 nm and Rpm of 733.9 ± 917.9 nm) were much higher than expected and greater than many of the average values reported in previous studies (Study 1 and Table 2.5). Thus, contact between the femoral component articulating surface and the baseplate on one condyle can cause severe damage to the condyle not experiencing wear through. This is likely caused by the generation of wear debris that then causes mode III wear to occur via the relocation of the wear debris to between the articulating surfaces of the non-wear through condyle.

During friction, the thin, passive oxide layer on the CoCrMo alloy surface, which is generally less than 10nm, is destroyed, exposing the non-oxidized metal. This non-

oxidized metal has a much higher surface free energy and chemical reactivity, possibly leading to greater contact adhesion. [43] This is one possible explanation of the mechanism of adhesion of titanium alloy to the articular surface of the cobalt chromium alloy following articulation caused by polyethylene wear through, as shown in Figure 3.7. Previous in vitro studies have reported the transfer of titanium debris to CoCrMo alloy surfaces when wear tests were conducted with high concentrations of titanium debris. [32] Small patches of the titanium were transferred to the harder CoCrMo alloy surface in the sliding direction, causing an increase in surface roughness of the worn CoCrMo alloy bearing surface. [32] This transfer of material causes increases in roughness of the articulating surface and the potentiality for generation of wear debris.

Oxidized zirconium alloy is thought to resist abrasive wear due to the high hardness of both the 4-5 μ m thick oxidized surface layer and the underlying metal alloy. [32] Oxide ceramics typically have a high wettability, which reduces the solid-solid contact during sliding and prevents the formation of a transfer layer. [32] The Oxinium component in the present study had the ceramic surface completely removed from the underlying metallic core. While there is little known about the exact mechanism of removal, it was likely caused by high contact stress, above the tensile strength of the oxidized zirconium surface, which caused the formation of cracks. Further exposure of the material to cyclic loading may have produced loading conditions above the fatigue strength of the oxidized zirconium alloy surface. The initial crack formation may have occurred when the femoral component contacted the tibial baseplate, though it is impossible to know if contact occurred before or after the removal of the surface. Due to

the high strength of the intramolecular bonding and gradient of oxidation of the zirconium, it is apparent that the surface was exposed to extremely elevated forces in order to remove the oxidized surface from the underlying zirconium alloy core.

Once a coating is penetrated, such as the oxidized layer of the zirconium alloy, the strength and hardness of the underlying bulk material determines the plastic deformation. [42] This explains the mechanism whereby the zirconium alloy was transferred to the surface of the titanium baseplate, as demonstrated in Figure 3.7. In addition, once the ceramic layer is destroyed, the pile-up of material at the edges of the indentation causes high stresses that could potentially lead to severe damage of the ceramic layer. [42]

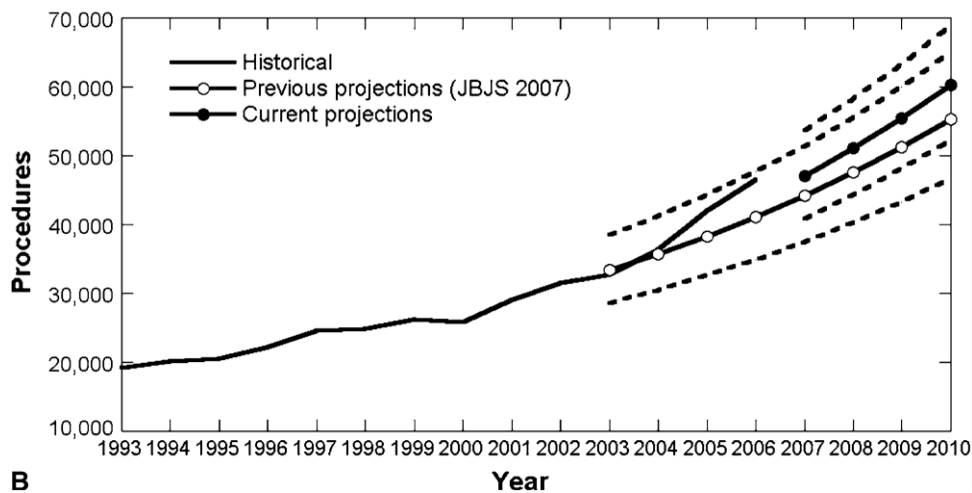
There were several limitations to this study. The sample size was very small with variations in prosthesis design of the femoral component, tibial insert and tibial baseplate, including size, geometry and manufacturing processes. There also were differences in surgical technique among surgeons. Not all combinations of potential bearing surfaces were considered and only a few samples were available for each type, further narrowing the sample size.

CHAPTER FOUR

STUDY 3: MODE IV WEAR MODEL

Introduction

As demonstrated by the previous two studies, wear and other factors contribute heavily to the success of joint arthroplasty. While it remains a very successful procedure overall, the number of revision surgeries being performed annually to replace failed TKA prostheses has continued to grow (Figure 4.1). [61] Kurtz, et al. projects that the number of revision TKA performed each year will increase by 601% from 2005 to 2030, [60] indicating the need to not only improve the longevity of primary TKA prostheses but also to improve revision TKA prosthesis designs to account for the more complex and varied knee geometries that remain following removal of the primary prosthesis.



B Figure 4.1: Historical incidence (1993-2006) and proposed projections of revision total knee arthroplasty in the U.S. The dotted lines represent the 95% confidence interval for the projections from the study [61]

The major challenge of revision surgery is the restoration of lost bone support and joint stability and alignment, which must be overcome to provide the support needed by the new prosthesis. [27, 37] The condition of the soft tissue, amount of available bone stock and joint stability play an important role in component selection during revision surgery. [83] Bone defects occurring with wear-induced osteolysis or with destructive revision surgery often require the use of bulk bone allografts and stemmed tibial components. [73] Cement and morcellized allograft can be used in small, contained tibial defects; however, allograft must be subjected to physiological loads and strains so fully cemented or press-fit long stems are often used to achieve these conditions and bypass the osseous defects. [27, 37, 83] In addition, it is often beneficial to use longer intramedullary stems to provide load sharing and subsequently decrease the amount of force transferred to the generally lacking, unstable bone stock of the proximal tibia. [27, 69]

In order to allow for greater intraoperative flexibility during the reconstruction of osseous defects, the stems commonly used in revision surgery are often modular in nature. [24, 59, 84] This allows surgeons to use varying designs and sizes of stems to address the various bone deficiencies that may not be fully appreciated pre-operatively. [69] Modularity also controls inventory costs for manufacturing companies and hospitals. [84] Modularity does, however, present with drawbacks, including the risk of dissociation, fretting at the junction, and increased cost of the prosthesis. [59] Modular prostheses have a greater potential for micromotion and fretting, increasing the potential for higher levels of metal debris. [32, 59] When Morse taper junctions are used to attach

modular components, decreasing the tolerances of the male and female parts of the taper minimizes micromotion and contact stresses at the junction. [84] Fretting can be extremely detrimental not only because it releases metallic ions and debris but also because it often leads to other corrosive processes. [82] Fretting at modular junctions specifically, can cause the removal of stable, passive oxide layers on metallic surfaces, which exposes the non-oxidized surface to harsh body fluids, releasing metal ions or debris. [82] Trapped fluid and debris between the modular interfaces, as well as micromotion, largely influence the occurrence of damage and corrosion at the junction. [67]

The micromotion and fretting that occurs at modular junctions would be considered mode IV wear, which is described as motion between two secondary bearing surfaces that were not intended to articulate by the designer. [14, 18, 70] The wear debris generated at these types of modular junctions is produced from both mechanical wear and corrosive wear and consists solely of metallic debris, though it has often been chemically altered. The ions that are released into the aqueous environment of the joint become metal-salt precipitates. [14] The metallic debris that is released can cause an increase in polyethylene wear via mode III wear or cause activation of macrophages and osteoclasts directly. [58] It is often associated with similar patient outcomes as polyethylene debris, including osteolysis and aseptic loosening. Radiolucent zones and osteolytic lesions are often visible on radiographs from patients with TKA prostheses experiencing motion at the modular junction.

Tibial components with intramedullary stems were initially designed to prevent tilting and liftoff of the baseplate when poor bone-stock in the proximal tibia was experienced. [20, 83, 86] Although stems are associated with higher stress shielding, there is little clinical relevance of this occurring in vivo. [83] The load transfer and stress shielding of short stem designs, often used in primary TKA, are primarily influenced by stem and prosthesis geometry, material of fabrication, tibial coverage and cementation techniques. [83] In general, the greater the difference in Young's modulus between the prosthesis and bone and the stiffer the material used for the tibial tray and stem, the greater the potential for stress shielding to be experienced by the surrounding bone. [83] The length of the stem determines the type of bone engaged; thus, the longer the stem the more likely cortical bone will be engaged, increasing stress shielding. [83] Shielding is greater in longer stems and fully cemented stems. [83]

Some tibial components are fixed with pegs (Figure 4.2), which can offer greater flexibility in positioning and potentially greater proximal tibia coverage in the absence of a stem. [20] It has been reported that pegs offer a lower and more uniform distribution of stress across the cement-bone interface, theoretically decreasing the chances of bone resorption and subsequent aseptic loosening. [20] Four-peg designs also have been shown to add considerable rotational stability under loading; however, pegs offer little assistance in malaligned patients, as they carry little to no moment to prevent liftoff. [88] Pegs have been associated with stress shielding of the proximal tibia; however, this tends to be very localized compared to central stems. [83] Pegged designs are often used in more active

and younger patients, while stemmed components are used in older, less active patients. [20]

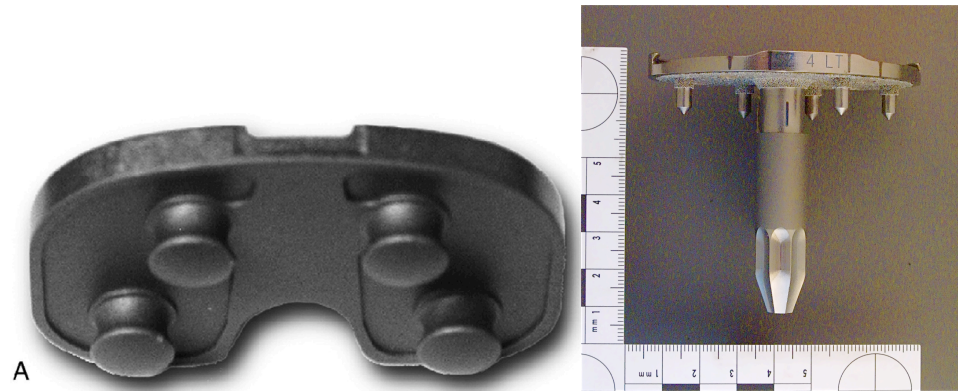


Figure 4.2: Representative images of tibial components that incorporate a pegged-only design (left) [20] and those that incorporate both pegs and a central stem (right)

Typically, tibial components that are both pegged and stemmed are used in patients with relatively poor bone stock. [20] However, in the present study, a TKA, which incorporates both a short, central cruciate stem and 5 pegs, was implanted consecutively in patients. The rationale for the use of this design was the pegs provided rotational stability and the stem prevented liftoff and added additional support. The only potential drawback of this particular design is the incorporation of a modular stem that attaches via a Morse taper. Modularity, while increasing flexibility during surgery, creates an additional possible wear source at the taper junction. Although, a study by Hardeman, et al. reported the Kaplan-Meier estimate of prosthesis survival at 5 and 10 years of cementless TKA with the particular design of the present study to be 98.2% and 97.1%, respectively, [46] there is still concern about possible wear at the modular junction of the tibial stem leading to prosthesis failure.

Stem performance will likely reflect the more varied loading and stress conditions that exist in revision TKA patients with progressive bone loss. Thus, modular tibial stems used in primary TKA present a “best case scenario” for prosthesis performance compared to modular stems used in revision TKA. The aim of the present study is to evaluate the clinical outcomes of 84 patients implanted with primary TKA prostheses of a single design (Profix Total Knee System, Smith and Nephew, Memphis, Tennessee) with a modular tibial stem. Due to the known potential for fretting and corrosion at modular junctions, the null hypothesis of the present study is that patients with TKA prostheses with modular stems will have greater biological evidence of reactive tissue, indicating these negative endpoints occurred, with higher revision rates compared to a prior study without modularity.

Materials and Methods

Between May 2001 and October 2002, 120 consecutive knees in 118 patients underwent primary TKA, using surface cementation, by Thomas Pace, M.D. All results were retrospectively reviewed in this institutional review board-approved study. Indication for TKA for all 118 patients was osteoarthritis. Patients with other indications received a different TKA design and are not included in this study. Nineteen patients were lost to death, while 2 patients were lost to follow-up. Only patients who achieved a minimum of 2 years of follow-up were evaluated, providing a final cohort of 85 knees in 84 patients. There were 60 females and 24 males, with an average age at index surgery of 66 ± 11 (31-86) years. Forty-seven of the TKA were implanted in the left knee and the remaining thirty-eight implanted in the right.

All patients were implanted with the same prosthesis design (Profix Total Knee System, Smith & Nephew, Memphis, TN) that incorporates a modular stem attached to the tibial baseplate (Figure 4.3). In the current study, tibial component geometry consisted of an asymmetric titanium alloy, porous tibial baseplate with a smooth surface-textured modular central stem and 5 peripheral pegs. This design provides the option for using one of four different central stems; however, all patients in the current study received the same smooth textured stem shown in Figure 4.3. Tibial components were fixed using a surface cementation technique with bone cement (Palacos R cement, Biomet Inc., Warsaw, IN) applied to the undersurface of the baseplate, excluding the pegs and stem. In 15 of the knees, the femoral component was composed of Oxinium (Smith & Nephew, Memphis, TN), while the remaining 70 knees had CoCrMo alloy femoral components. The tibial inserts were all fabricated from UHMWPE that had been sterilized in ethylene oxide. All but two patients were implanted with a conforming plus tibial insert design, which also is known as an anterior-constrained design. The other two patients received a standard conforming tibial insert.

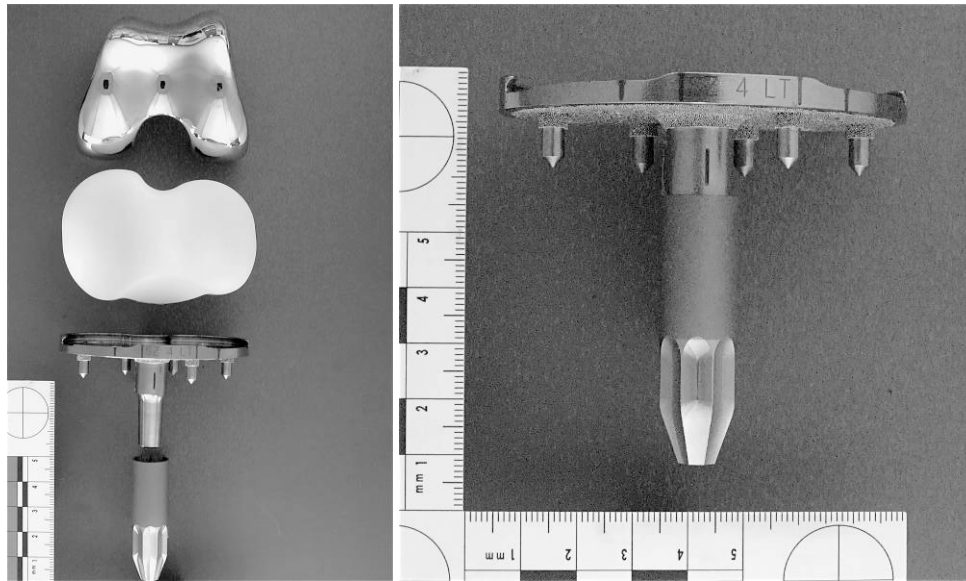


Figure 4.3: Gross photographs of each individual component of Profix TKA (left) and assembled tibial component with stem of current study (right)

Available records were retrospectively reviewed to assess clinical and radiographic outcomes. The surgical approach and posterior cruciate ligament treatment (retention or sacrificed) were recorded, as well as preoperative and post-operative Knee Society Scores, [56] and postoperative range of motion (ROM). Any noted complications or subsequent revision surgeries were considered. Radiographic analysis consisted of two independent observers assessing full-length, long-standing anteroposterior, sunrise and lateral views (Figure 4.4) and recording the presence of osteolytic lesions and any radiolucent lines, greater than 2mm, located under the surface-cemented tibial tray.

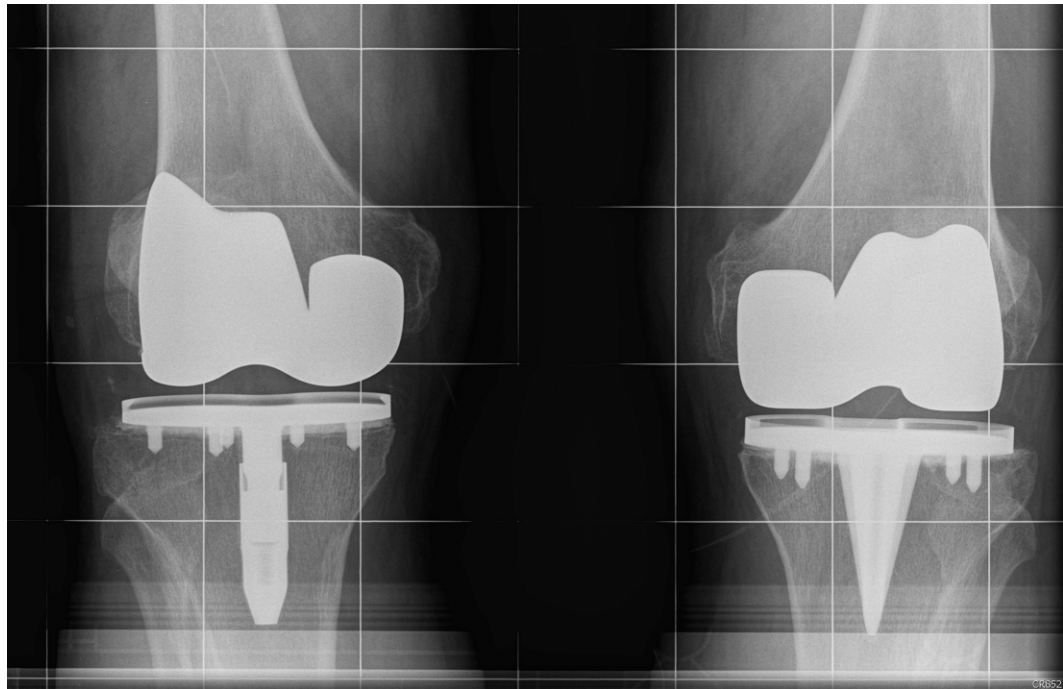


Figure 4.4: Radiograph with Profix Total Knee System (left) and Natural Knee (right)

Prior Study Case

This level III therapeutic study involved patients of the present study treated with a primary TKA with a modular tibial stem being compared to a systematic review of prior studies in which patients were treated with a non-modular primary TKA. A study of primary TKA with surface cemented non-modular stemmed tibial components by Hofmann, et al. was chosen as the prior study, and data were taken directly from the published manuscript. [55] This prior study was chosen because the TKA evaluated (Natural Knee II, Zimmer, Warsaw, IN) is similar to the present study TKA (Profix Total Knee System). Similarities in design include the use of an asymmetric titanium tibial base plate with a central cruciate stem and peripheral pegs. The main difference in design

between studies is the modularity of the tibial stem in the present study. Similar to the study population, tibial components were fixed using a surface cementation technique with bone cement (Simplex P cement, Howmedica, Rutherford, NJ) impregnated with 1.2g of Tobramycin per 40g of cement applied to the undersurface of the tibial baseplate.

Hofmann, et al. reported a retrospective review of 128 consecutive knees in 109 patients that were implanted between 1991 and 1998 with primary surface cemented TKA and had a minimum of 5-year follow-up. Preoperative diagnosis, range of motion (ROM), Modified Hospital of Special Surgery (HSS) Score, Knee Society Score and radiographic data were analyzed. In addition, surgical technique, posterior cruciate ligament treatment, and posterior ROM, HSS score and alignment data were recorded. Radiographic data included alignment, radiolucent lines and osteolytic lesions evaluated on full-length 52-inch long standing, anteroposterior, lateral, and sunrise views. Hofmann, et al. defined osteolysis as an expanding area of focal radiolucency of at least 1cm.

Of the 128 knees in 109 patients, 2 were lost to follow-up and 19 unilateral patients died before the 5-year follow-up, leaving 107 knees in 88 patients for review. Eighteen male and seventy females were included in the study with an average age of 74 (range 46-91) years. Forty of the knees were implanted into the left knee and forty-eight into the right.

Results

Eighty-five knees received primary, cemented TKA in eighty-four patients and were analyzed in the current study. The posterior cruciate ligament (PCL) was sacrificed in all 85 cases, with antero-posterior stability provided through the use of the conforming plus polyethylene insert, which incorporates an anterior-constrained design. The subvastus approach was used in 83 (97.6%) of the cases, whereas the remaining 2 (2.4%) were exposed using the medial parapatellar approach. The subvastus approach was selected on a case by cases basis with the premise that it may offer some benefit by allowing a quicker recovery and less post-operative pain. It was performed on patients if the distal thigh circumference was small enough that it could practically be done; however, patients with a larger distal thigh circumference received the medial parapatellar approach.

The average follow-up was 81.6 ± 37.6 (23.8-133.2) months. Average pre-operative Knee Society Scores were 78.6 ± 4.6 (70-87) and improved to 99.2 ± 2.0 (90-100) postoperatively. Postoperative ROM averaged $118.5^\circ \pm 5.4^\circ$ (95° - 128°) of flexion.

No radiographs demonstrated osteolytic lesions around the tibial component. Radiolucent lines adjacent to 2 TKA were noted upon initial radiographic analysis. In one TKA, the radiolucent line was less than 2mm in thickness, asymptomatic and not associated with prosthesis failure. In the other TKA, a 2mm lucent line was noted and further investigated as the patient had indicated mild pain. The pain was most recently indicated to be mild patellofemoral pain, most likely related to the un-resurfaced patella, and is not considered to be associated with failure of the tibial component.

None of the knees included in the current study required revision surgery. No infections were recorded in this series of patients. One knee experienced dehiscence and was treated accordingly. Finally, one knee required closed, manual manipulation following implantation because the average flexion was less than 120° at the 3 month follow-up visit.

Prior Study Case

Of the 107 knees in 88 patients, the preoperative diagnosis included 76 knees with primary osteoarthritis, 10 with rheumatoid arthritis and 2 with post-traumatic. Thirty-five of the PCL's were spared and the remaining 53 were sacrificed, with subsequent anteroposterior stabilization provided by the use of an ultracongruent/deep-dish polyethylene tibial insert, which incorporates an anterior-constrained design. The subvastus approach was used in 67 knees, while 21 knees received the medial parapatellar approach.

Average follow-up for the prior study was 95 (range 63-155) months. Post-operative Knee Society Scores averaged 195 (range 162-200), which improved from the pre-operative scores that averaged 122 (range 94-152). Post-operative range of ROM for all knees averaged 1°-116°.

Based on the radiographic review of this prior study, osteolytic lesions were not reported for any TKA. However, three TKA had non-progressive radiolucent lines adjacent to the tibial baseplate, which all were asymptomatic and not associated with prosthesis failure. Two other TKA required revision surgery but none of the tibial components were revised for loosening. One revision consisted of a polyethylene

exchange due to PCL insufficiency and the other required a femoral component removal due to pain and possible loosening at 4 years following index surgery. No infections were recorded in this study. The overall survivorship at an average of 95 months was 98%.

Discussion

In the present series, patients that underwent surface cemented primary TKA with a modular stemmed tibial baseplate experienced excellent functional outcomes with few complications and no revisions. Of the two patients with radiolucent lines, one was less than 2 mm and asymptomatic, while the other presented with patellofemoral pain, indicating the complications were likely not related to the tibial component but rather the un-resurfaced patella.

In this level III therapeutic study, both patient cohorts were treated with similar surgical approaches, including surface cementation, and were implanted with similar asymmetric, pegged tibial baseplates with a central stem. While the focus of the prior study was tibial fixation, the present study aimed to determine if tibial component modularity in primary TKA induces biological evidence indicative of fretting and corrosion, and higher revision rates. It is well accepted that the first roentgenographic indication of wear and micromotion is a radiolucent zone between the bone and cement mantle, indicating the presence of a fibrous membrane. [4, 73] Moreover, also it has been reported that 31 months is the average time it takes for osteolysis to present itself radiographically. [44] For these reasons, the present study includes patients with a minimum of 2-year follow-up in order to capture this time point indicating wear and osteolysis.

The lack of radiolucent lines and osteolysis in these TKA indicates that fretting and corrosion were not prominent features at the modular junction. The modular tibial stem design obtained similar and acceptable patient outcomes in comparison to non-modular tibial components of a similar design. The absence of revision and lack of tibial component-related complications implies that modularity in this short-stemmed design should not be associated with increased risk of osteolysis or loosening and subsequent prosthesis failure.

There are several limitations to this study. Although the Hofmann, et al. study had a slightly larger number of patients compared to the sample size of the present study, we believe the data are comparable, due to the common surgical techniques and tibial component design. Additionally, the prior study did not present the data in a way that allowed for statistical comparison of patient outcome measures, but the number of revisions and complications, as well as the post-operative ROM indicates similar patient outcomes for both studies.

CHAPTER FIVE
ENGINEERING SIGNIFICANCE

Study 1: Mode I Wear

These empirical studies provide data that fit within a theoretical framework related to material properties and bearing performance. Archard's wear law (1953) is the primary theoretical model used to calculate the amount of polyethylene wear debris generated in knee prostheses.

$$V = K \times P \times X$$
$$K = (Ra)^{n>1}$$

Figure 5.1: Archard's wear law

The model states that the volume of material removed, V (mm^3), is directly related to the normal load, P (N), the sliding distance, X (mm) and the wear factor, K ($\text{mm}^3\text{N}^{-1}\text{m}^{-1}$). [35] The normal load, P (N), is related to the patient's body weight and activity. D'Lima, et al. reported on peak forces experienced by the knee during various activities, including walking at different speeds, biking, playing tennis, walking up stairs, and several others. [29, 30] The peak tibial forces were reported to be between 2 and 5 times body weight, depending on the activity. The sliding distance, X (mm) is primarily related to the activity level of the patient, which determines the number of gait cycles a prosthesis must complete. DesJardins, et al. studied the kinematic travel distance per gait cycle of TKA and determined that approximately 20mm is traveled by the medial condyle per gait cycle, [33] assuming that the average person will complete about 1 million cycles per year. The wear factor, K ($\text{mm}^3\text{N}^{-1}\text{m}^{-1}$), is the final theoretical

contributor to volumetric wear, and it is directly related to the measured surface roughness of the femoral counter-bearing surface. [35] The wear factor is an empirical value that should be determined for each system and material being tested, so the relationship of surface roughness to the wear factor varies with different materials and lubricants.

Archard's wear law has long been the standard theoretical model used to determine volumetric wear in TKA; however, there are several assumptions made by the model that often make it less predictive of in vivo function. First, the equation assumes constant material properties, which polyethylene does not possess. Under different loading conditions, polyethylene demonstrates non-linear behavior. [62] In addition, in order to estimate an appropriate k-value for the Archard's equation, it is necessary to know the polyethylene wear associated with the different roughness values measured. This relationship can be obtained from controlled tribology assessments. [38] In this manner, the surface topographies of both bearing surfaces impact the wear debris generation at the articular surface. This pathway of using retrieved components to provide more specific roughness measures and therefore more specific estimates of the k-value, have shown promise in previous wear modeling studies. [40] The model considers joint loading to play a role in wear, which is directly related to the contact stress and contact pressure existing between the two surfaces. Considering that contact stress can vary on the macro-scale (conformity and alignment of the prostheses) and on the micro-scale (real contact area dependent on surface asperities), the measures of surface roughness generated in this thesis would be expected to impact the latter case (Figure 5.2

and 5.3). Therefore, these data provide a broader representation of the real-world parameters useful for making the Archard's law more predictive of in vivo bearing performance. The data produced by Study 1 provides realistic values for surface roughness measured after in vivo function. Based on the data of Study 1, the wear factor would vary greatly due to such large ranges of measured values for surface roughness. This would in turn, lead to volumetric wear of varying degrees.

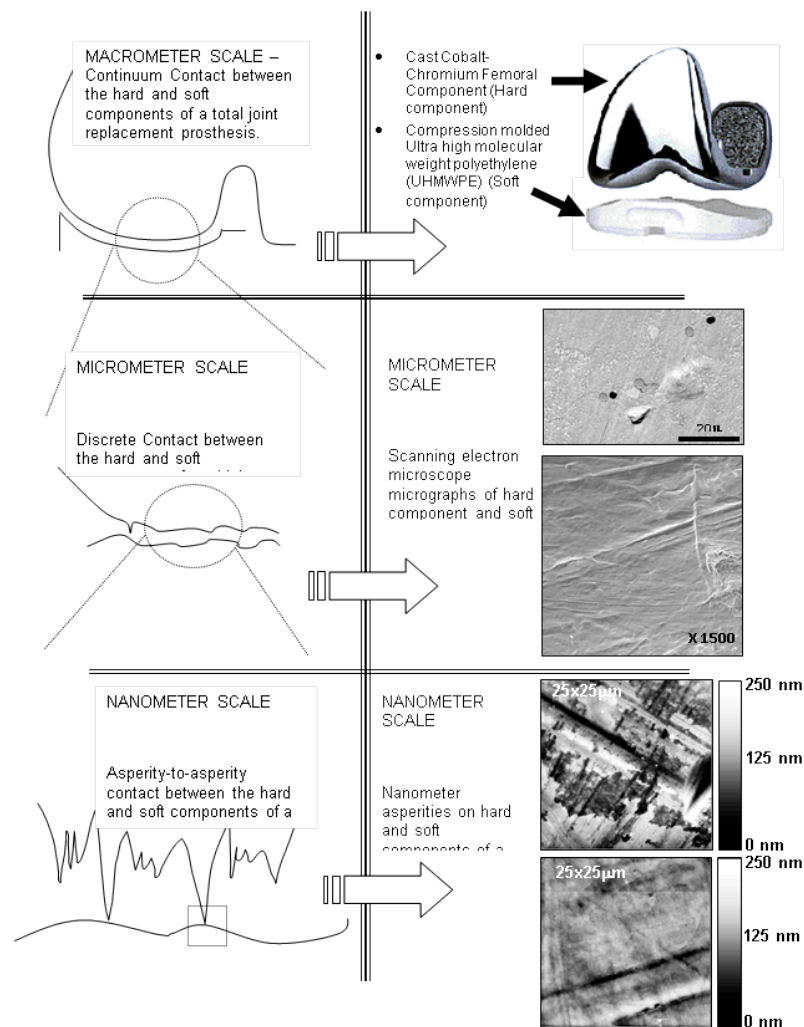


Figure 5.2: Description of different scales to consider when characterizing contact between two bearing surfaces in TKA

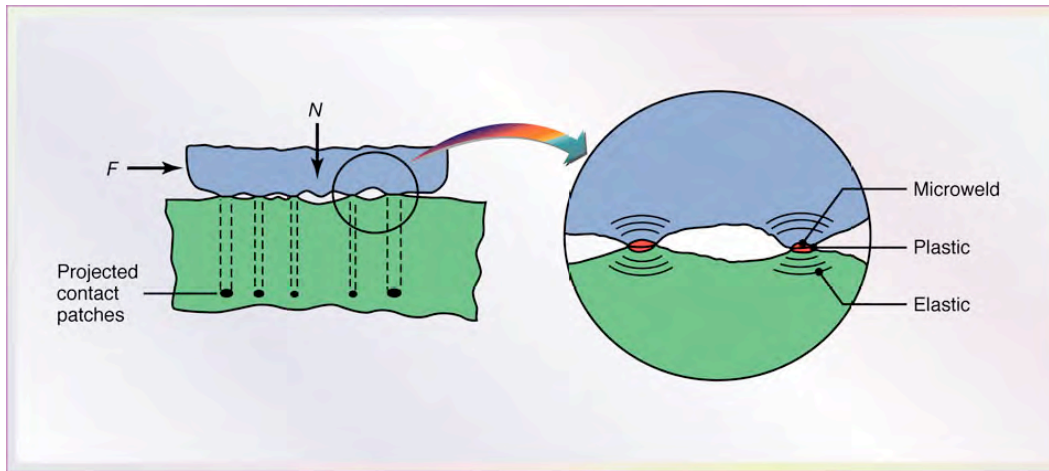


Figure 5.3: Simplified cartoon demonstrating real contact area between two bodies in contact

Study 2: Mode II Wear

Study 2 demonstrated the catastrophic failure of TKA that resulted from complete polyethylene wear through leading to contact between the articular surface of the femoral component and metallic tibial baseplate. It is possible that excessive contact stresses likely contributed to such extreme polyethylene wear. Contact stress on the macro-scale is largely determined by conformity of the bearing surfaces and thickness of the polyethylene. [17] Therefore, the Hertz contact stress model is a suitable theoretical framework for these observations.

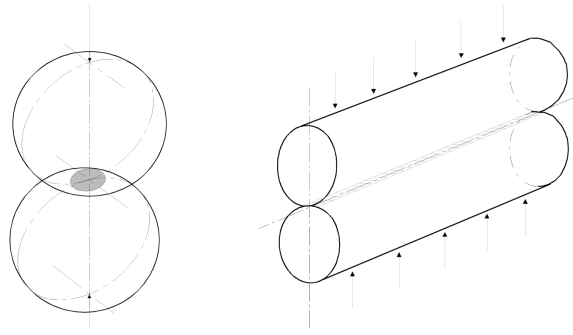


Figure 5.4: Representative image of point (left) and line (right) contact determined by shape and conformity of bearing surfaces

	Parallel Cylinder - Line Contact	Spheres - Circular Point Contact
Parameters	Contact half-width a Load per unit width, P Material Properties, E_1, ν_1, E_2, ν_2 Contact radii, R_1, R_2	Circle of radius a Applied load, P Material Properties, E_1, ν_1, E_2, ν_2 Contact radii, R_1, R_2
Dimensions of the contact	$a = \sqrt{\frac{4PR}{\pi E^*}}$	$a = \sqrt[3]{\frac{3PR}{4E^*}}$
Relative radius of curvature, R	$\frac{1}{R} = \frac{1}{R_1} + \frac{1}{R_2}$	
Reduced modulus ³ , E^*	$\frac{1}{E^*} = \frac{1 - \nu_1^2}{E_1} + \frac{1 - \nu_2^2}{E_2}$	
Contact pressure distribution, p	$p(x) = p_0 \sqrt{1 - \frac{x^2}{a^2}}$	$p(r) = p_0 \sqrt{1 - \frac{r^2}{a^2}}$
Mean contact pressure, p_m Max contact pressure, p_0	$p_m = \frac{\pi p_0}{4} = \frac{P}{2a}$	$p_m = \frac{2p_0}{3} = \frac{P}{\pi a^2}$
Line Contact	Point Contact	
$\frac{\sigma_x}{p_0} = -\sqrt{1 - \frac{x^2}{a^2}}$	$\frac{\sigma_r}{p_0} = \left(\frac{1 - 2\nu}{3}\right) \left(\frac{a^2}{r^2}\right) \left\{ 1 - \left(1 - \frac{r^2}{a^2}\right)^{3/2} \right\} - \left(1 - \frac{r^2}{a^2}\right)^{1/2}$	
$\frac{\sigma_y}{p_0} = -2\nu \sqrt{1 - \frac{x^2}{a^2}}$	$\frac{\sigma_\theta}{p_0} = -\left(\frac{1 - 2\nu}{3}\right) \left(\frac{a^2}{r^2}\right) \left\{ 1 - \left(1 - \frac{r^2}{a^2}\right)^{3/2} \right\} - 2\nu \left(1 - \frac{r^2}{a^2}\right)^{1/2}$	
$\frac{\sigma_z}{p_0} = -\sqrt{1 - \frac{x^2}{a^2}}$	$\frac{\sigma_z}{p_0} = -\sqrt{1 - \frac{r^2}{a^2}}$	

Table 5.1: The top part of the table demonstrates the equations to determine contact area and contact pressure of both line and point contacts. The bottom part of the table shows the equations to find the surface stresses of the different contacts within the contact region

The Hertz model states that contact pressure is directly related to contact area (a) and the load applied (P). Furthermore, contact area is dependent on the contact radii (R), the elastic moduli (E), and the Poisson's ratio (ν) of both bearing materials. As such, the contact pressure in a point contact condition is greater than line contact when loading and material properties are held constant. The model also states that surface stresses are related to contact pressure (P), contact area (a), axis of symmetry (r) and Poisson's ratio (ν) depending on the type of contact, as well as, the direction of stress. For this thesis, the majority of prostheses had a round on flat conformity, which is modeled using a point contact. However, it should be noted that assumptions for using Hertz equation are not always met with in vivo knee joint function. During in vivo function, smooth frictionless surfaces are not necessarily present and it cannot be assumed that polyethylene exhibits exclusively elastic behavior, since both plastic deformation and creep are likely to occur.

Kuster, et al. has reported contact stresses at the tibial plateau during different activities much higher than the yield range of polyethylene, indicating an increased risk of polyethylene failure (Figure 5.5). [63] While the exact cause of the failure of the polyethylene bearings in Study 2 is unknown, excessive contact stresses above the stress yield of polyethylene is a likely explanation.

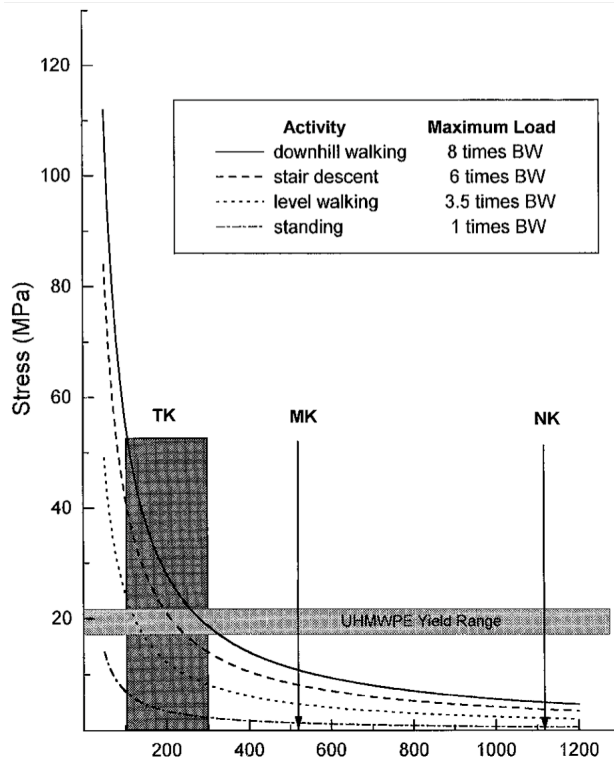


Figure 5.5: Tibial plateau stress versus contact area for different daily activities for a 70kg female. Uniform stress distribution is assumed. The horizontal bar indicates the yield range of polyethylene while the vertical bars demonstrate the range of tibiofemoral contact area of tested knee prostheses (TK), a knee joint after meniscectomy (MK) and a natural knee joint (NK) [63]

On the micro-scale contact stress is primarily determined by surface roughness and asperities on the surfaces of both articular bearings, which are reflected in the roughness values generated in this thesis. Therefore, to understand the mechanisms of complete wear-through evident in these bearings, it necessarily requires both macro and micro conditions to be modeled. The data from Study 2 provides realistic values for surface roughness values for TKA that have experienced in vivo function that resulted in polyethylene wear through.

Study 3: Mode IV Wear Model

While Morse tapers have been successfully used to assemble the individual components of modular prosthesis in joint replacement, there is concern associated with the potential of the taper to produce wear debris and corrosion products. The use of Morse tapers originated in machine tooling as a means to provide frictional rotary coupling in milling machines and drill presses. [41] The machine tool tapers are available in a variety of dimensions and angles, that typically range from 2° to 8°, which are dependent on the company manufacturing them. [41] Most orthopaedic tapers have angles between 4° and 6° and dimensions that are much shorter than industrial Morse tapers. [59] The tapers are composed of male and female parts, also known as the trunion, or tapered shank, and the bore, or socket, respectively, which are mechanically interlocked by elastic deformation and stabilized by friction to form a cold weld. [24, 41, 59, 84] Since the tapers are not standardized, the components may appear to be compatible but actually are not, so extreme care must be taken by the surgeon to ensure that different manufacturers' products are not mixed and that proper sizing is used. [41]

The fit of the trunion and bore, as well as the longevity of the connection, can be affected by surface finish, composition, and design tolerances. [41] It has been suggested that long-term fixation of the interlocking Morse taper junction in prostheses is enhanced by extracortical bone bridging and ingrowth, since bone formation around the taper lock can decrease the stresses transmitted by the joint to reduce fatigue and metal wear. [24] Some of the known problems associated with Morse tapers are fretting and corrosion at the interface. The common types of corrosion reported at modular junctions have

included galvanic, fretting and crevice, resulting in ion release and debris generation. Corrosion can occur at the modular junction due to the difference in oxygen concentration at the trunion-bore interface when compared to the outside of the prosthesis. [41] Collier, et al. reported that corrosion occurred when a stagnant and acidic aqueous collection of bodily fluids formed at the taper interface. [25] In addition, the repeated removal of the passivating layer on the outside of the metallic materials through micromotion, or fretting, also causes the modular junction to experience corrosion. [41, 67] Galvanic corrosion mechanisms have been noted in some cases with taper interfaces having different metallic compositions of the trunion and bore. [67, 82] In addition to the polyethylene wear mechanisms discussed in Chapters 2 and 3, fretting and corrosion at Morse taper junctions can activate an aggressive host response leading to osteolysis and loosening of TJA prostheses.

In addition to corrosion, dissociation of the Morse taper junction is another problem that can lead to catastrophic failure of implanted prostheses. This failure is often mediated by contamination of the interlock with fluids or debris during intraoperative taper assembly, especially PMMA and bone, machining mismatch, corrosion, and trauma. [59] Studies have shown that as little as 0.4mL of bodily fluids or water can prevent proper seating of the taper and inhibit the frictional fit. [59] Kung-Hua Chu, et al. reported that a Ti/Ti combination for the taper lock couple resulted in the greatest minimization of the risk of fatigue fracture, while a Co/Co combination provided the least risk of fluid inflow and corrosion of the junction. [24] Under normal loading conditions, the cold weld at the modular junction is stable and would require excessive forces for

dissociation to occur. [59] Distraction forces for metallic TKA femoral components with a Morse taper junction are reported to be greater than 431kg (950 lbs), which is significantly greater than forces experienced by tapers in normal in vivo loading. [59] However, any machining mismatch in the bore and trunion interface can cause significant decreases in distraction forces for these tapers. [59] Off axis loading, typically caused by trunion-bore mismatch or manufacturing tolerances, can compromise the cold weld of a Morse taper by increasing micromotion and contact stresses, often leading to failure. [59, 84]

Morse tapers provide a successful means of interlocking modular components of TJA prostheses to allow surgeons to have greater intra-operative flexibility and hospitals to maintain a reduced inventory. Despite all of the concerns associated with fretting, corrosion and dissociation, Study 3 demonstrated that positive clinical outcomes can be obtained with the use of modular prostheses. While some surgeons may be hesitant to expose patients to another potential wear source, none of the patients in Study 3 have experienced endpoints associated with the common concerns of fretting, corrosion, or dissociation. Therefore, Study 3 provides some context for interpreting taper corrosion that can exist on retrieved components with modular junctions, and a baseline clinical study for understanding modular junction performance in less optimal physiological conditions, such as poor bone support after revision arthroplasty.

CHAPTER SIX

CONCLUSIONS & FUTURE STUDIES

Retrieval studies provide great value in understanding in vivo performance of prostheses, as well as providing endpoints for basic science studies. The types of studies help provide data that make in vitro simulator and analytical models more predictive of in vivo performance. Using surface roughness assessments provide insight into failure mechanisms of TJA; however, even in the most simplified wear equation (Archard's law), joint loading and activity level likely dominate the vastly different wear presentations that are observed in retrieved prostheses from varying patients. Despite our best efforts in designing TJA prostheses, catastrophic failures still occur, as seen in Study 2. Trying to gain further insight about the risk and mechanisms of failure, gives both engineers and material scientists the tools needed to mitigate these risks when designing future devices. The ultimate goal is to achieve positive clinical outcomes and improve patients' quality of life, which can only be achieved by designing successful prostheses for a wide range of pathologies and patient types.

The purposes of Studies 1 and 2 discuss bearing surface interactions and the potential generation of wear debris, specifically in relation to mode I and mode II wear. Mode I wear is well known to be the greatest contributor to debris generation in well-fixed, stable prostheses. Dowson, et al. determined that the volumetric wear of polyethylene was related to the applied load, sliding distance, and a wear factor that is an exponential function of measured surface roughness. [35] While measures of increased surface roughness of the femoral counter-bearing surface may predict increases in

polyethylene wear, Study 1 demonstrates that in vivo duration does not necessarily correlate with increased surface roughness or the associated polyethylene wear area. In addition, femoral components experience a wide range of damage modes following in vivo service. The present study not only characterized the distribution of the damage modes, showing that scratching resulted in the greatest damage coverage across the articular surface, but also that each mode corresponds to a different range of surface roughness values. These variations in surface roughness lead to dramatic differences in the damage modes experienced by the corresponding polyethylene insert. Further studies are needed to determine how femoral component damage modes, and the mechanisms that caused them, play a role in polyethylene damage mode and volume of debris produced.

Mode II wear occurs much less frequently than mode I wear; however, it has been a concern for many decades and continues to lead to revision, as seen by Study 2. This mode of wear in the knee, represents the extreme failure cascade that involves complete polyethylene wear through of the tibial insert leading to contact between the femoral articular surface and the metallic tibial baseplate. This phenomenon not only causes increased roughening on the articular surface exposed to the wear through, but also leads to greater damage and roughening of the non-wear through condyle. Wear through is commonly associated with increased wear debris that is composed of both polyethylene and metallic debris. Study 2 demonstrates that the material properties, such as hardness and tensile strength, of both the tibial baseplate and femoral component play an integral role in determining the roughness and mode of damage on the articular femoral surface.

While oxidized zirconium was introduced to decrease bearing surface wear and resist the abrasion and scratching damage often experienced by the titanium and cobalt chromium alloys, it may be more susceptible to cracking and macroscopic removal when exposed to high contact stresses. Future studies, with greater sample sizes, are needed to further investigate the influence of material properties on femoral component damage modes, specifically in situations of mode II wear.

The purpose of Study 3 discusses potential wear debris generation at modular junctions, specifically in relation to mode IV wear. Modularity in TKA is beneficial in reducing inventory and giving surgeons intraoperative flexibility to better handle unforeseen complications in the reconstruction of osseous defects often prevalent in revision. However, it also introduces a new potential source of wear debris. This debris can be generated mechanically, as well as from varying corrosive processes possible at the modular junction. While modular stem designs are often utilized in revision TKA, recent primary TKA prostheses also have incorporated modularity. This introduced a new concern for metallic wear generation in primary TKA, which was the focus of Study 3. Using a prior study, this study was able to demonstrate that surface cemented modular short-stemmed tibial components performed just as successfully as non-modular tibial components of a similar design. This study only reviewed one particular design; however, it demonstrates that modularity does not always increase the risk of wear leading to osteolysis and/or loosening and subsequent revision. Despite all of the concerns with modularity, Study 3 demonstrated that clinical outcomes can be positive. However, further studies are needed to better assess modularity in less optimal conditions, such as

when bone stock has been destroyed, either by pathological processes or during revision surgery. The outcomes of Study 3 provide control data for further studies of modular junction performance under less optimal conditions. In general, the conditions that lead to failure or success of the modular junction should be studied in further detail.

REFERENCES

1. Affato S, Leardini W, Rocchi M. Investigation on Wear of Knee Prostheses Under Fixed Kinematic Conditions. *Artificial Organs*. 2007;32:13–18.
2. Alvarez E, DesJardins JD, Schmitt S, Harman MK. Relationship between Surface Roughness and Articular Wear for Cobalt-Chrome on Polyethylene Bearing Couples: Evaluation of Retrieved Unicondylar Knee Replacements. In: *58th Annual Meeting of the Orthopaedic Research Society*. San Francisco; 2012.
3. Alvarez E, Harman MK, DesJardins JD. Development and assessment of knee femoral components surface damage classification and training method. In: *58th Annual Meeting of the Orthopaedic Research Society*. San Francisco; 2012.
4. Amstutz HC, Campbell P, Kossovsky N, Clarke IC. Mechanisms and Clinical Significance of Wear Debris-Induced Osteolysis. *Clinical Orthopaedics and Related Research*. 1992;276:7–18.
5. Anon. ASTM F1472-08: Standard Specification for Wrought Titanium-6Aluminum-4Vanadium Alloy for Surgical Implant Applications. 2008:1–5.
6. Anon. ASTM F1108-04: Standard Specification for Titanium-6Aluminum-4Vanadium Alloy Castings for Surgical Implants. 2009;04:1–4.
7. Anon. ASTM F648-10a: Standard Specification for Ultra-High-Molecular-Weight Polyethylene Powder and Fabricated Form for Surgical Implants. 2010:1–8.
8. Anon. ASTM F2384-10: Standard Specification for Wrought Zirconium-2 .5Niobium Alloy for Surgical Implant Applications (UNS R60901). 2010:1–4.
9. Anon. ASTM F1537-11: Standard Specification for Wrought Cobalt-28Chromium-6Molybdenum Alloys for Surgical Implants. 2011:1–4.
10. Anon. *Swedish Knee Arthroplasty Register Annual Report 2012*. Lund; 2012.
11. Anon. National Joint Registry for England and Wales. 2012.
12. Anon. ASTM F75-12: Standard Specification for Cobalt-28 Chromium-6 Molybdenum Alloy Castings and Casting Alloy for Surgical Implants. 2012:1–4.
13. Anon. Newport Orthopedic Institute. 2013. Available at: http://hipknee arthritis.com/2010/05/12/rotating-platform-knee-replacement-one-system-many-option-for-total-knee-replacement/rotating_illustration/.

14. Archibeck MJ, Jacobs JJ, Roebuck KA, Glant TT. The Basic Science of Periprosthetic Osteolysis. *The Journal of Bone and Joint Surgery*. 2000;82-A:1478–1489.
15. Banks S a, Harman MK, Bellemans J, Hodge W a. Making sense of knee arthroplasty kinematics: news you can use. *The Journal of Bone and Joint Surgery*. 2003;85-A Suppl:64–72.
16. Bartel DL, Burstein AH, Santavicca EA, Insall JN. Performance of the Tibial Component in Total Knee Replacement. *The Journal of Bone and Joint Surgery*. 1982;64-A:1026–1033.
17. Bartel DL, Rawlinson JJ, Burstein AH, Ranawat CS, Flynn Jr. WF. Stresses in Polyethylene Components of Contemporary Total Knee Replacements. *Clinical Orthopaedics and Related Research*. 1995;317:76–82.
18. Bauer TW, Schils J. The pathology of total joint arthroplasty.II. Mechanisms of implant failure. *Skeletal Radiology*. 1999;28:483–497.
19. Bert JM, Reuben J, Kelly F, Gross M, Elting J. The incidence of modular tibial polyethylene insert exchange in total knee arthroplasty when polyethylene failure occurs. *The Journal of arthroplasty*. 1998;13:609–14.
20. Bertin KC. Tibial component fixation in total knee arthroplasty: a comparison of pegged and stemmed designs. *The Journal of arthroplasty*. 2007;22:670–8.
21. Brach Del Prever EM, Bistolfi A, Bracco P, Costa L. UHMWPE for arthroplasty: past or future? *Journal of orthopaedics and traumatology: official journal of the Italian Society of Orthopaedics and Traumatology*. 2009;10:1–8.
22. Burnell CDC, Brandt J-M, Petrak MJ, Bourne RB. Posterior condyle surface damage on retrieved femoral knee components. *The Journal of arthroplasty*. 2011;26:1460–7.
23. Callahan CM, Drake BG, Heck D a, Dittus RS. Patient outcomes following unicompartmental or bicompartamental knee arthroplasty. A meta-analysis. *The Journal of arthroplasty*. 1995;10:141–50.
24. Chu Y, Elias JJ, Duda GN, Frassica FJ, Chao EY. Stress and micromotion in the taper lock joint of a modular segmental bone replacement prosthesis. *Journal of biomechanics*. 2000;33:1175–9.

25. Collier JP, Surprenant VA, Jensen RE, Mayor MB, Surprenant HP. Corrosion between the components of modular femoral hip prostheses. *The Journal of bone and joint surgery British volume*. 1992;74:511–517.
26. Collier MB, Engh CA, Engh G a. Shelf Age of Polyethylene Tibial Component and Outcome of Unicondylar Knee Arthroplasty. *The Journal of Bone and Joint Surgery*. 2004;86:763–769.
27. Completo a, Simões J a, Fonseca F, Oliveira M. The influence of different tibial stem designs in load sharing and stability at the cement-bone interface in revision TKA. *The Knee*. 2008;15:227–32.
28. Cooper JR, Dowson D, Fisher J. Macroscopic and microscopic wear mechanisms in ultra-high molecular weight polyethylene. *Wear*. 1993;162:378–384.
29. D’Lima DD, Patil S, Steklov N, Colwell CW. The 2011 ABJS Nicolas Andry Award: Lab”-in-a-Knee: In Vivo Knee Forces, Kinematics, and Contact Analysis. *Clinical Orthopaedics and Related Research*. 2011;469:2953–2970.
30. D’Lima DD, Steklov N, Patil S, Colwell CW. The Mark Coventry Award: in vivo knee forces during recreation and exercise after knee arthroplasty. *Clinical Orthopaedics and Related Research*. 2008;466:2605–2611.
31. Davidson JA, Asgian CM, K MA, Kovacs P. Zirconia (ZrO₂)-coated zirconium-2.5Nb alloy for prosthetic knee bearing applications. *Bioceramics*. 1992;5:389–401.
32. Davidson JA, Poggie RA, Mishira AK. Abrasive Wear of Ceramic, Metal, and UHMWPE Bearing Surfaces from Third-Body Bone, PMMA Bone Cement, and Titanium Debris. *Bio-Medical Materials and Engineering*. 1994;4:213–229.
33. DesJardins JD, Banks S a, Benson LC, Pace T, LaBerge M. A direct comparison of patient and force-controlled simulator total knee replacement kinematics. *Journal of Biomechanics*. 2007;40:3458–3466.
34. DesJardins JD, Burnikel B, LaBerge M. UHMWPE wear against roughened oxidized zirconium and CoCr femoral knee components during force-controlled simulation. *Wear*. 2008;264:245–256.
35. Dowson D, Taheri S, Wallbridge NC. The role of counterface imperfections in the wear of polyethylene. *Wear*. 1987;119:277–293.

36. Dwyer KA, Topoleski LD, Bauk DJ. The Neglected Side of the Wear Couple: Analysis of Surface Morphology of Retrieved Femoral Components. In: *39th Annual Meeting of the Orthopaedic Research Society*. San Francisco; 1993.
37. Engh G a, Herzworm PJ, Parks NL. Treatment of major defects of bone with bulk allografts and stemmed components during total knee arthroplasty. *The Journal of bone and joint surgery. American volume*. 1997;79:1030–9.
38. Fisher J, Dowson D, Hamdzah H, Lee HL. The effect of sliding velocity on the friction and wear of UHMWPE for use in total artificial joints. *Wear*. 1994;175:219–225.
39. Fisher J, Firkins P, Reeves EA, Hailey JL, Isaac GH. The influence of scratches to metallic counterfaces on the wear of ultra-high molecular weight polyethylene. *Proceedings of the Institution of Mechanical Engineers , Part H: Journal of Engineering in Medicine*. 1995;209:263–264.
40. Fregly BJ, Sawyer WG, Harman MK, Banks S a. Computational wear prediction of a total knee replacement from in vivo kinematics. *Journal of biomechanics*. 2005;38:305–14.
41. Friedman RJ, Black J, Galante JO, Jacobs JJ, Skinner HB. Current Concepts in Orthopaedic Biomaterials and Implant Fixation. *The Journal of Bone and Joint Surgery*. 1993;75-A:1086–1109.
42. Galetz MC, Fleischmann EW, Konrad CH, Schuetz A, Glatzel U. Abrasion resistance of oxidized zirconium in comparison with CoCrMo and titanium nitride coatings for artificial knee joints. *Journal of biomedical materials research. Part B, Applied biomaterials*. 2010;93:244–51.
43. Galetz MC, Seiferth SH, Theile B, Glatzel U. Potential for adhesive wear in friction couples of UHMWPE running against oxidized zirconium, titanium nitride coatings, and cobalt-chromium alloys. *Journal of biomedical materials research. Part B, Applied biomaterials*. 2010;93:468–75.
44. Gupta SK, Chu A, Ranawat AS, Slamin J, Ranawat CS. Osteolysis after total knee arthroplasty. *The Journal of arthroplasty*. 2007;22:787–99.
45. Hailey JL, Fisher J, Dowson D. A tribological study of a series of retrieved Accord knee explants. *Medical engineering & physics*. 1994;16:223–228.
46. Hardeman F, Vandenuecker H, Van Lauwe J, Bellemans J. Cementless total knee arthroplasty with Profix: a 8- to 10-year follow-up study. *The Knee*. 2006;13:419–21.

47. Harman M, Cristofolini L, Erani P, Stea S, Viceconti M. A pictographic atlas for classifying damage modes on polyethylene bearings. *Journal of Materials Science: Materials in Medicine*. 2011;22:1137–1146.
48. Harman MK, Affatato S, Spinelli M. Polyethylene insert damage in unicondylar knee replacement: a comparison of in vivo function and in vitro simulation. *Proceedings of the Institution of Mechanical Engineers , Part H: Journal of Engineering in Medicine*. 2009;224:822–830.
49. Harman MK, Banks S a, Hodge WA. Organization of a postmortem implant retrieval program in a community hospital setting. In: *Transactions of the 67th Annual Meeting of the American Academy of Orthopaedic Surgeons*. Orlando; 2000:610.
50. Harman MK, Banks S a, Hodge WA. Polyethylene damage and knee kinematics after total knee arthroplasty. *Clinical Orthopaedics and Related Research*. 2001;392:383–393.
51. Harman MK, DesJardins JD, Benson LC. Comparison of Polyethylene Tibial Insert Damage from In Vivo Function and In Vitro Wear Simulation. *Journal of Orthopaedic Surgery*. 2008;27:540.
52. Harman MK, Schmitt S, Rössing S, Banks S a, Sharf H-P, Viceconti M, Hodge WA. Polyethylene damage and deformation on fixed-bearing, non-conforming unicondylar knee replacements corresponding to progressive changes in alignment and fixation. *Clinical biomechanics (Bristol, Avon)*. 2010;25:570–5.
53. Heyse TJ, Chen DX, Kelly N, Boettner F, Wright TM, Haas SB. Matched-pair total knee arthroplasty retrieval analysis: oxidized zirconium vs. CoCrMo. *The Knee*. 2011;18:448–52.
54. Hirakawa K, Jacobs JJ, Urban R, Saito T. Mechanisms of Failure of Total Hip Replacements: Lessons Learned From Retrieval Studies. *Clinical Orthopaedics*. 2004:10–17.
55. Hofmann A a, Goldberg TD, Tanner AM, Cook TM. Surface cementation of stemmed tibial components in primary total knee arthroplasty: minimum 5-year follow-up. *The Journal of arthroplasty*. 2006;21:353–7.
56. Insall JN, Dorr LD, Scott RD, Scott WN. Rationale of the Knee Society clinical rating system. *Clinical Orthopaedics and Related Research*. 1989;248:13–14.
57. Jacobs JJ, Roebuck KA, Archibeck MJ, Hallab NJ, Glant TT. Osteolysis: Basic Science. *Clinical Orthopaedics and Related Research*. 2001;393:71–77.

58. Jones DM, Marsh JL, Nepola J V, Jacobs JJ, Skipor a K, Urban RM, Gilbert JL, Buckwalter J a. Focal osteolysis at the junctions of a modular stainless-steel femoral intramedullary nail. *The Journal of bone and joint surgery. American volume*. 2001;83-A:537–48.
59. Kennedy JG, Kearns SR, Quinlan WB. Dissociation of a Morse-Taper Stemmed Tibial Component Following Revision Total Knee Arthroplasty: a case report. *The Journal of Bone and Joint Surgery*. 2003;85-A:536–538.
60. Kurtz S, Ong K, Lau E, Mowat F, Halpern M. Projections of primary and revision hip and knee arthroplasty in the United States from 2005 to 2030. *The Journal of Bone and Joint Surgery*. 2007;89:780–785.
61. Kurtz SM, Lau E, Ong K, Zhao K, Kelly M, Bozic KJ. Future Young Patient Demand for Primary and Revision Joint Replacement: National Projections from 2010 to 2030. *Clinical Orthopaedics and Related Research*. 2009;467:2606–2612.
62. Kurtz SM, Pruitt L, Jewett CW, Crawford RP, Crane DJ, Edidin a a. The yielding, plastic flow, and fracture behavior of ultra-high molecular weight polyethylene used in total joint replacements. *Biomaterials*. 1998;19:1989–2003.
63. Kuster MS, Wood G a, Stachowiak GW, Gächter A. Joint load considerations in total knee replacement. *The Journal of bone and joint surgery British volume*. 1997;79-B:109–113.
64. Lakdawala a, Todo S, Scott G. The significance of surface changes on retrieved femoral components after total knee replacement. *The Journal of bone and joint surgery. British volume*. 2005;87:796–9.
65. Lancaster JG, Dowson D, Isaac GH, Fisher J. The wear of ultra-high molecular weight polyethylene sliding on metallic and ceramic counterfaces representative of current femoral surfaces in joint replacement. *Proceedings of the Institution of Mechanical Engineers, Part H: Journal of Engineering in Medicine*. 1997;211:17–24.
66. Levesque M, Livingston BJ, Spector M. Scratches on Condyles in Normal Functioning Total Knee Arthroplasty. In: *44th Annual Meeting of the Orthopaedic Research Society*. New Orleans; 1998.
67. Lieberman JR, Rimnac CM, Garvin KL, Klein RW, Salvati E a. An analysis of the head-neck taper interface in retrieved hip prostheses. *Clinical orthopaedics and related research*. 1994:162–7.

68. Lonner JH, Klotz M, Levitz C, Lotke P a. Changes in bone density after cemented total knee arthroplasty: influence of stem design. *The Journal of arthroplasty*. 2001;16:107–11.
69. Mabry TM, Vessely MB, Schleck CD, Harmsen WS, Berry DJ. Revision total knee arthroplasty with modular cemented stems: long-term follow-up. *The Journal of arthroplasty*. 2007;22:100–5.
70. McKellop HA, D’Lima D. How have wear testing and joint simulator studies helped to discriminate among materials and designs? *The Journal Of The American Academy Of Orthopaedic Surgeons*. 2008;16 Suppl 1:S111–S119.
71. Mundermann A, Dyrby CO, D’Lima DD. In Vivo Knee Loading Characteristics during Activities of Daily Living as Measured by an Instrumented Total Knee Replacement. *Journal of Orthopaedic Research*. 2008;26:1167–1172.
72. Muratoglu OK, Burroughs BR, Bragdon CR, Christensen S, Lozynsky A, Harris WH. Knee Simulator Wear of Polyethylene Tibias Articulating against Explanted Rough Femoral Components. *Clinical Orthopaedics and Related Research*. 2004;428:108–113.
73. Naudie DDR, Ammeen DJ, Engh G a, Rorabeck CH. Wear and osteolysis around total knee arthroplasty. *The Journal Of The American Academy Of Orthopaedic Surgeons*. 2007;15:53–64.
74. Newman J, Pydisetty R V, Ackroyd C. Unicompartmental or total knee replacement: the 15-year results of a prospective randomised controlled trial. *The Journal of bone and joint surgery. British volume*. 2009;91:52–7.
75. Parikh A, Morrison M, Jani S. Wear Testing of Crosslinked and Conventional UHMWPE Against Smooth and Roughened Femoral Components. In: *53rd Annual Meeting of the Orthopaedic Research Society*. San Diego; 2007.
76. Perry J. *Gait Analysis: Normal and Pathological Function*. Thorofare: Slack, Inc. 1992.
77. Que L, Topoleski LD. Surface roughness quantification of CoCrMo implant alloys. *Journal of biomedical materials research*. 1999;48:705–11.
78. Reis MD, Salehi A, Widding K, Hunter G. Polyethylene Wear Performance of Oxidized Zirconium and Cobalt Chrome Knee Components Under Abrasive Conditions. In: *American Academy of Orthopaedic Surgeons Annual Meeting*. Dallas; 2002.

79. Ries MD, Salehi A, Widding K, Hunter G. Polyethylene wear performance of oxidized zirconium and cobalt-chromium knee components under abrasive conditions. *The Journal of bone and joint surgery. American volume*. 2002;84-A Suppl:129–35.
80. Saikko V, Calonijs O, Keränen J. Effect of counterface roughness on the wear of conventional and crosslinked ultrahigh molecular weight polyethylene studied with a multi-directional motion pin-on-disk device. *Journal of biomedical materials research*. 2001;57:506–12.
81. Saldanha K a N, Keys GW, Svard UCG, White SH, Rao C. Revision of Oxford medial unicompartmental knee arthroplasty to total knee arthroplasty - results of a multicentre study. *The Knee*. 2007;14:275–9.
82. Schaaff P. The role of fretting damage in total hip arthroplasty with modular design hip joints -evaluation of retrieval studies and experimental simulation methods. *Journal of applied biomaterials & biomechanics : JABB*. 2004;2:121–35.
83. Scott CEH, Biant LC. The role of the design of tibial components and stems in knee replacement. *The Journal of Bone and Joint Surgery*. 2012;94-B:1009–1015.
84. Shareef N, Levine D. Effect of manufacturing tolerances on the micromotion at the Morse taper interface in modular hip implants using the finite element technique. *Biomaterials*. 1996;17:623–30.
85. Smith B, Schlachter A, Ross M. Pin on Disk Wear Testing of Scratched Engineered Surface. In: *55th Annual Meeting of the Orthopaedic Research Society*. Las Vegas; 2009.
86. Stern SH, Wills D, Gilbert JL. The Effect of Tibial Stem Design on Component Micromotion in Knee Arthroplasty. *Clinical Orthopaedics and Related Research*. 1997;345:44–52.
87. Tingstad EM. Total Knee & Partial Knee Replacement Surgery. 2009. Available at: <http://www.inlandortho.net/education1.html>.
88. Walker PS, Hsu HP, Zimmerman R a. A comparative study of uncemented tibial components. *The Journal of arthroplasty*. 1990;5:245–53.
89. White SE, Whiteside LA, McCarthy DS, Anthony M, Poggie RA. Simulated Knee Wear with Cobalt Chromium and Oxidized Zirconium Knee Femoral Components. *Clinical Orthopaedics and Related Research*. 1994;309:176–184.